RSC Advances

REVIEW

View Article Online
View Journal | View Issue

Cite this: *RSC Adv.*, 2021, **11**, 250

Recent advances in the synthesis and applications of mordenite zeolite – review

S. Narayanan,*[a] P. Tamizhdurai,*[b] V. L. Mangesh,[c] C. Ragupathi,[a] P. Santhana krishnan[d] and A. Ramesh[d]

Among the many industrially important zeolites, mordenite is found to be interesting because of its unique and exceptional physical and chemical properties. Mordenite (high silica zeolite) is generally prepared by the hydrothermal method using TEA^+ cations. TEA^+ cations are the best templating agent, though they can create a number of issues, for instance, generating poison and high manufacturing cost, wastewater contamination, and environmental pollution. Hence, it is necessary to find a mordenite synthesis method without using an organic template or low-cost template. In this review, a number of unique sources were used in the preparation of mordenite zeolite, for instance, silica sources (rice husk ash, silica gel, silica fumes), alumina sources (metakaolin, faujasite zeolite) and sources containing both silica and alumina (waste coal fly ash). These synthesis approaches are also based on the absence of a template or low-cost mixed organic templates (for instance, glycerol (GL), ethylene glycol (EG), and polyethylene glycol 200 (PEG)) or pyrrolidine-based mesoporogen (*N*-cetyl-*N*-methylpyrrolidinium) modifying the mordenite framework which can create unique properties. The framework properties and optical properties (indium-exchanged mordenite zeolite) have been discussed. Mordenite is generally used in alkylation, dewaxing, reforming, hydrocracking, catalysis, separation, and purification reactions because of its large pore size, strong acidity, and high thermal and chemical stability, although the applications are not limited for mordenite zeolite. Recently, several applications such as electrochemical detection, isomerization, carbonylation, hydrodeoxygenation, adsorption, biomass conversion, biological applications (antibacterial activity), photocatalysis, fuel cells and polymerization reactions using mordenite zeolite were explored which have been described in detail in this review.

Received 6th November 2020
Accepted 23rd November 2020

DOI: 10.1039/d0ra09434j

rsc.li/rsc-advances

Introduction

Catalysis, particularly heterogeneous catalysis, represents an essential part in the sustainable synthesis of numerous chemical compounds (which includes specialty, fine and commodity chemicals, and also pharmaceutical products) and renewable generation of fuels and energy, which are among the most crucial concepts of green chemistry (in other words, the ninth concept catalytic reagents (as selective as possible) are better than stoichiometric reagents[1]).

At present, around 90% of chemical production procedures and over 20% of most commercial products are based on catalytic pathways.[2] In heterogeneous catalysis, porous materials have gained a prominent place. Porous materials have contributed considerably to the current progress of chemical processes. Porous materials can be utilized either as catalyst supports or catalysts. For instance, in petrochemistry, the application of microporous crystalline zeolites being a catalyst has considerably increased the selectivity, quality, and yield of the products in the following reactions (for example isomerization, alkylation, and cracking). In general the lifetime of the catalytic materials is higher, and in the meantime, the consumption of energy reduces.[3]

Porous materials are usually solid substances, although not restricted to solids these days.[4] Porous materials could possibly be classified into three kinds according to their pore size. The pore size less than 2 nm and between 2–50 nm were called microporous and mesoporous materials. The pore size of more than 50 nm were called macroporous materials. This is according to the IUPAC classification (1960) based on the nitrogen adsorption experiment.[5] This can also be categorized based on the nature of solid phases (for example, amorphous or crystalline) or building blocks. Fig. 1 shows the classification of porous materials by their pore size, nature of phase, and building blocks.

[a]*Sriram College of Arts and Science, Perumalpattu, Veppampattu, Tiruvallur, Tamilnadu, 602024, India. E-mail: essarrenn@gmail.com; Tel: +91-9566225479*

[b]*Environmental and Water Resources Engineering Division, Department of Civil Engineering, Indian Institute of Technology Madras, Chennai-600036, India. E-mail: tamizhvkt2010@gmail.com; Tel: +91-9677146579*

[c]*Department of Marine Engineering, Coimbatore Marine College, Coimbatore-641035, India*

[d]*Department of Chemistry, College of Engineering, Guindy, Anna University, Chennai 600025, India*

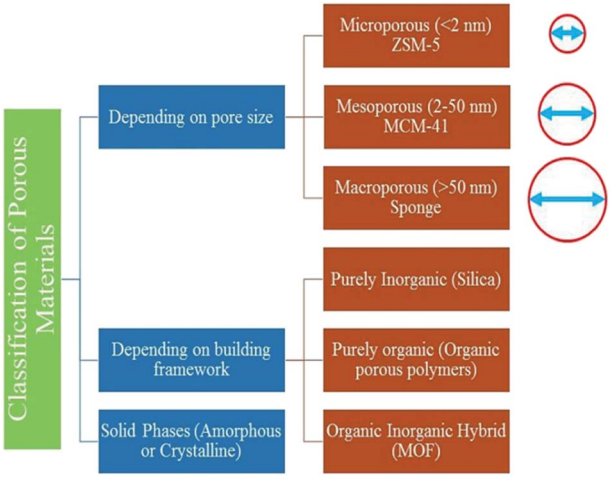

Fig. 1 Classification of porous materials.

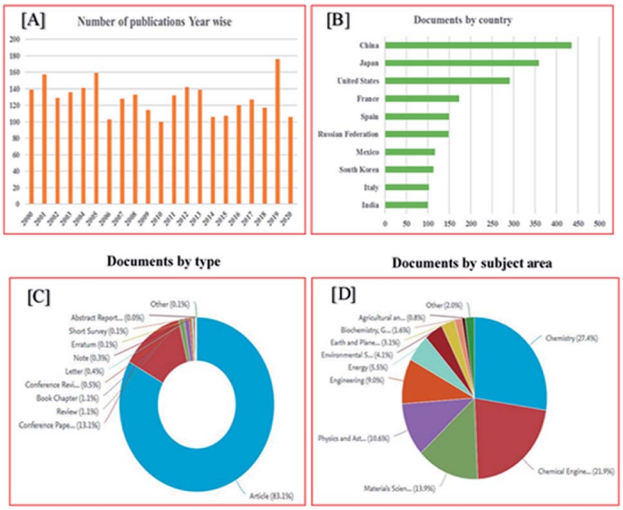

Fig. 2 Statistical data related to publications of mordenite zeolite (obtained from Scopus as of March 2019). Mordenite research article published (A) year-wise (B) country-wise (C) article type-wise (D) subject-wise.

Zeolites tend to be common in our present lifestyle because they are utilized for a wide variety of applications which includes agriculture,[6] gas adsorption,[7] green chemistry,[8,9] water treatment,[10–12] petroleum refining,[13] animal feed additives,[14] and additionally several others. Zeolites can be formed naturally[15,16] or prepared in a laboratory.[17] To date, 234 zeolites with different structural types have been identified. Zeolites are a class of inorganic aluminosilicates having a consistent framework structure assembled by corner-sharing units of silicates (SiO_4) and aluminates (AlO_4) in a number of fractions however having a silicon to aluminum ratio (Si/Al) more than one.[18] In zeolites the SiO_4 and AlO_4 units are connected together in different modes, creating a huge collection of zeolites having distinctive pore sizes (typically less than 1 nm) as well as pore topologies.[5] The International Zeolite Association assigned distinctive three-letter codes for these crystalline microporous materials, for example, BEA (Zeolite Beta), FAU (Faujasite) and MOR (Mordenite), *etc.* These materials have different physical as well as chemical properties. Of these zeolites, about 20 are industrial-operated, however exclusively five are known as "Big Five" zeolites, for example, BEA, FAU, FER, MOR, and MFI,[19] because of their importance in the present chemical industry, in particular, conversions of petrochemical, for instance, the production of propylene, gasoline (volatile, flammable liquid hydrocarbons), and aromatics productions (for example, ethylbenzene and cumene).

Mordenite is among the list of an important class of zeolites and most common exploitable deposits of natural zeolites and is often an important component.[20,21] Mordenite belongs to a large-pore zeolite and behaves as a molecular sieve (two-dimensional) for tiny molecules such as nitrogen and oxygen and for larger molecules being one-dimensional zeolite.[22] It shows better chemical resistance, greater thermal stability, contains both Brønsted and Lewis acid sites, a large quantity of pore volume, and high surface area.[23] Because of these kinds of properties, mordenite is employed in many industrial processes for example methylamine synthesis, disproportionation, trans-alkylation, and hydroisomerization.[24] Though the application of mordenite zeolite not limited as mentioned above and it is growing each year. For this reason, the purposes of the present review started to significantly assess the mordenite zeolite synthesis with a novel approach, properties, and most recent application. Also, an extensive review article found for ZSM-5 and not for mordenite zeolite which have almost the same properties. Fig. 2A–D showing statistical data related to publications of mordenite zeolite between 2000–2020 (based on the Scopus statistics).

In two decades, 2711 documents were published and each year more than 100 articles were published related to mordenite. In 2019 a maximum of 176 documents was published and in 2020 till now, 106 documents were published (Fig. 2A). It will become higher compared to 2019 and in previous years. This indicates an increase in the importance of the mordenite zeolite. Fig. 2B displays the contribution to mordenite by country-wise. China, Japan, and the United States contributed a lot in the field of mordenite synthesis and applications. From Fig. 2C we can understand 83.1% (2254) of documents out of 2711 documents published as research articles. Though only 31 documents (1.1%) were published in review article type and the last 10 years only 15 review articles only published. Fig. 2D showing a list of publications based on the subject area. The subject area chemistry, engineering, chemical engineering, material science, physics, and astronomy contributed more. It should be noted that the contribution of mordenite in energy also in considerable numbers which indicates the importance of energy-related applications. From the above statistical data, we understand the importance of mordenite zeolite still maintaining and growing rapidly from 2019. Hence writing a review article on mordenite provides a better idea to readers with respect to mordenite synthesis and applications.

Experimental

Synthesis of mordenite zeolite by a novel approach

We know, typically the mordenite zeolite can be synthesized by a hydrothermal approach using templates. In this section, we

will discuss the synthesis of mordenite zeolite using a novel approach which was not widely discussed. The summary of the synthesis of the mordenite zeolite is presented in Table 1.

Rice husk ash

In 2020 earlier, Klunk and his collaborators synthesized mordenite zeolite using rice husk ash as silicon source and metakaolin for aluminium source.[25] They modified the mordenite synthesis without using organic templates according to the reported synthesis by Costa and Araujo.[26] By using X-ray fluorescence (XRF), they find the composition of rice husk ash (RHA) and metakaolin. The major component present in RHA is SiO_2 (90.02%) and in metakaolin, the major components are SiO_2 (48.27%), Al_2O_3 (35.34%), and some other oxides in a few percent. The mordenite zeolites with different Si/Al ratios (5, 10, 15, and 20) were prepared by varying amounts of RHA and metakaolin. The typical synthesis procedure of mordenite is explained here. Initially, 3.5 mol L^{-1} of NaOH dissolved in the water and split into two parts (500 ml). The required amount of RHA dissolved in one part and metakaolin in another part. Then both the solutions mixed together and kept at room temperature for the sol–gel process followed by drying in an oven at 90 °C for 24 h. Finally, the solid product calcinated at 550 °C for 6 h. They also calculated product yield. The mordenite with Si/Al ratio 5 and 20 yields of 73% (both) product, Si/A ratio 15, and 10 yields 71% and 70% respectively. The total BET surface area and microporous pore volume decrease from 347 $m^2\ g^{-1}$ and 0.279 $cm^3\ g^{-1}$ to 314 $m^2\ g^{-1}$ and 0.198 $cm^3\ g^{-1}$ with a decreasing Si/Al ratio from 20 to 5. The mesopore volume present in a negligible amount and also decreases from 0.03 $cm^3\ g^{-1}$ to 0.01 $cm^3\ g^{-1}$ with an increasing Si/Al ratio from 20 to 5. They carried out the thermogravimetric analysis and found as-synthesized materials are stable up to 400 °C. The stability decreases with increasing the Si/Al ratio from 20 to 5. In conclusion, the mordenite with Si/Al ratio has a higher surface area, high thermal stability, and a highly crystalline nature than the other materials.[25] However, the material stability should be improved, and also the mesopore volume to be increased for synthesizing hierarchical pore structures to use this material in various applications effectively.

Waste coal fly ash

Nowadays researchers focused on the synthesis of catalytic materials from waste sources. For example, waste coal fly ash is one of the waste materials generated by thermal power stations. Hence, researchers start using coal fly ash for the preparation of zeolites. Lankapati *et al.* synthesized mordenite using waste coal fly ash based on the concept of Lathiya *et al.* used waste coal fly ash as a solid acid catalyst by converting into sulfated fly ash.[27,28] The authors (Lankapati *et al.*) utilized the mordenite catalyst as an absorbent towards the removal of metal ions. They prepared mordenite zeolite using coal fly ash based on the composition reported by Kim *et al.* with some changes.[29] Kim *et al.* utilized silica and sodium aluminate for silica and alumina sources, whereas Lankapati *et al.* used waste coal fly ash for silica and alumina sources as an alternative for commercial sources. The utilization of coal fly ash makes the mordenite zeolite process becomes sustainable, economical, and greener approach. Only the outlined procedure gave also by Kim *et al.* The required amounts of silica and alumina source dissolved in sodium hydroxide and subjected to crystallization at 150 to 170 °C using stainless steel tube having a capacity of 100 ml with autogenous pressure. Finally, the product calcinated at 700 to 1200 °C. The composition ratio of 0.1–1.6 Na_2O/SiO_2 : 7–150 SiO_2/Al_2O_3 : 100–190 H_2O/Na_2O.[29] From BET analysis, the total surface area and total pore volume of 133 $m^2\ g^{-1}$

Table 1 Summary of synthesis of mordenite zeolite

S. no.	Title	Source for silica and alumina	Template	Reaction conditions	Reference
1	Rice husk ash	Rice husk ash (RHA) and metakaolin	Absence	Room temperature for sol–gel process; calcinated at 550 °C for 6 h	25
2	Waste coal fly ash	Waste coal fly ash for both	No information	Crystallization at 150 to 170 °C	27
3	Silica gel/low-cost mixed organic templates	Silica gel and aluminum nitrate	Low-cost mixed organic templates (glycerol (GL), ethylene glycol (EG), polyethylene glycol 200 (PEG))	Crystallization at 180 °C for 2 days; calcinated at 550 °C for 2 h	30
4	Silica fume (microsilica)	Silica fume and metakaolin	Absence	Heated for 24 h at 180 °C in a Teflon reactor; no calcination	31
5	Faujasite/*N*-cetyl-*N*-methylpyrrolidinium (C16NMP)	Sodium silicate and faujasite zeolite	Pyrrolidine-based mesoporogen	Crystallization at 140 °C for 6 days with stirring (50 RPM); calcined at 550 °C for 10 h	32
6	Ball milling, solvent-free synthesis	Sodium silicate, SiO_2, $Al_2(SO_4)_3 \cdot 18H_2O$	Absence	In an oven for 24, 48, or 72 h at 180 °C	33
7	Ultrafast, organic structure-directing agent-free synthesis	40 wt% LUDOX HS-40 (colloidal silica) and $NaAlO_2$	Absence	Heated at 210 °C in an oil bath	38
8	Piperazine as OSDA	Ludox AS-40 and $NaAlO_2$	Piperazine	Hydrothermally treated at 150 °C for 72 h to 192 h	43

and 0.090 $cm^3\ g^{-1}$, which is lower than commercial mordenite have the surface area and total pore volume of 432 $m^2\ g^{-1}$ and 0.200 $cm^3\ g^{-1}$. Though mesopore volume was found to be higher prepared by waste coal fly ash 0.060 $cm^3\ g^{-1}$ than commercial mordenite (0.020 $cm^3\ g^{-1}$) which is necessary for absorption applications. They concluded, the waste coal fly ash can be a potential alternative and cost-effective source for the preparation of porous zeolites as absorbents.

Silica gel/low-cost mixed organic templates

In mid-2019, Abdelrahman *et al.* synthesized mordenite nanoparticles through a hydrothermal approach by employing cost-effective organic templates such as glycerol (GL), ethylene glycol (EG), polyethylene glycol 200 (PEG). The templates used in various combinations, for instance, all the three templates (GL–EG–PEG) simultaneously or used any two templates. The two combinations are GL–EG, GL–PEG, and EG–PEG respectively. The standard procedure for the fabrication of mordenite zeolite is done as follows. Initially, two sets of solutions were prepared. The first solution contains, 12.0 g NaOH, 9.22 g silica gel dissolved in 325 ml double distilled water. The second solution contains, 0.53 g of aluminum nitrate dissolved in 75 ml double distilled water. The second solution added drop-wise into the first solution with stirring for 1 h. The resulting gel heated hydrothermally in a stainless steel autoclave for 2 days at 180 °C. Before the hydrothermal process, 5 ml organic templates (fixed quantity for all templates) were added. After the end of the reaction, the autoclave cooled, the contents filtered and washed with double distilled water several times. Finally, the samples were dried at 100 °C for 6 h, followed by calcination at 550 °C for 2 h. These catalysts were used in the removal of Pb(II) ions from the aqueous solutions. From XRD analysis, it is found that the mordenite prepared by EG–PEG and GL–EG–PEG showed a smaller crystallite size of 38.75 and 45.96 nm compared to mordenite prepared by GL–PEG and GL–EG crystallite size of 86.78 and 98.70 nm, respectively which is also confirmed by HR-TEM. Various morphological change happened by changing template combinations. The mordenite prepared by using EG–PEG has a higher surface area (27.590 $m^2\ g^{-1}$) and pore volume (0.0470 $cm^3\ g^{-1}$) compared to others and as a result, mordenite prepared by EG–PEG achieved efficient removal of Pb(II) ions (17.40 mg g^{-1}) from the aqueous solutions. They studied kinetic, pH, equilibrium, thermodynamic, desorption, and reusability studies.[30] To obtain higher surface area and pore volume this process needs to be tailored for multi-purpose applications.

Silica fume (microsilica)

In the early-2019, Chen *et al.* synthesized efficient and environment-friendly monolithic mordenite (seed-assisted) nanostructures without using organic structure-directing agents. The authors used silica fume (microsilica) and metakaolin for silicon source and aluminium source respectively. The major component present in silica fume is SiO_2 (93.11%) and in metakaolin, the major components are SiO_2 (55.06%), Al_2O_3 (44.12%), and some other oxides in a few percent. The typical synthesis procedure is explained here. Initially, the silica fume and mordenite mixed well with the mordenite seed for 5 min in a pulp mixture. The alkali (NaOH) solutions were mixed with the above mixture with continuous stirring for obtaining uniformed slurry. The slurry cast into molds and then sealed in a plastic bag. Followed by kept in an oven for 24 h at 50 °C for the curing process. The obtained geopolymer block was placed with distilled water (75 ml) and heated for 24 h at 180 °C in a Teflon reactor for hydrothermal synthesis. Finally, the nanostructured monolithic mordenite formed. The as-synthesized mordenite has a total surface area and total pore volume of 30.16 $m^2\ g^{-1}$ and 0.063 $cm^3\ g^{-1}$.[31] This is a cost-effective process and eco-friendly process for mordenite zeolite. However, the authors not tested any applications with the monolithic mordenite. Hence, the efficiency of the material needs to be tested, and based on that the properties of the material should be improved.

Faujasite/*N*-cetyl-*N*-methylpyrrolidinium (C16NMP)

In 2019, Bolshakov and his collaborators prepared mordenite nanorods using cheap pyrrolidine-based mesoporogen. The typical synthesis procedure of mordenite as follows. Initially, the *N*-cetyl-*N*-methylpyrrolidinium (bromide form – C16NMP) dissolved in deionized water. Then, a solution of sodium silicate has been added into a solution of C16NMP drop-wise and then stirred for 15 min at room temperature. Subsequently, the desired amount of NH_4Y zeolite (faujasite) was added to the above solution. The resultant gel vigorously stirred for 90 min at room temperature and then transferred into a Teflon-lined stainless-steel autoclave. The above mixture was heated at 140 °C for 6 days with stirring (50 RPM). The obtained product filtered, washed completely with deionized water. The product dried at 110 °C in an air oven and finally calcined at 550 °C for 10 h. The synthesis mixture having a molar composition of x C16NMP: $2.47Na_2O$; $0.33Al_2O_3$; $10SiO_2$; $256H_2O$. The composition of x is varied (x = 0.15, 0.20, 0.25, 0.30, 0.35, 0.40). For comparison purposes, mordenite zeolite is prepared without using C16NMP. The mordenite zeolite with C16NMP composition 0.15 has the highest surface area (392.8 $m^2\ g^{-1}$), whereas mordenite zeolite with C16NMP composition 0.25 has the highest external surface area (88.5 $m^2\ g^{-1}$) and total pore volume (0.23 $cm^3\ g^{-1}$) even though it contains a total surface area of 379.3 $m^2\ g^{-1}$. The synthesized materials were tested in the hydroisomerization of alkane and showed better selectivity compared to bulk mordenite zeolite.[32]

Ball milling, solvent-free synthesis

In the mid-2019, Nada *et al.* synthesized mordenite and ZSM-5 zeolites through template-free and solvent-free approach, and also no crystals seed were added. Also, the reaction was carried out by the mechanochemical pathway (ball-milling).[33] In recent times, the mechanochemical approach gained importance and was used in the preparation of solid-state materials, mixed-halide perovskites, transition-metal porphyrins.[34–36] The as-synthesized materials were tested in the conversion of glucose and cellulose into hydroxymethylfurfural and their catalytic

performance is comparable to commercial and ZSM-5 zeolites. In a typical synthesis, 5.03 mmol $Na_2SiO_3 \cdot 9H_2O$, 24 mmol SiO_2, 0.98 mmol $Al_2(SO_4)_3 \cdot 18H_2O$, NaOH were taken as silica, alumina source, and an additive. At 1400 RPM, the above solid mixture was grinded by a ball mill (high energy) for 25 min and 50 min. Then, the contents were transferred into Parr autoclave (Teflon lined). Subsequently, the autoclaved placed in an oven for 24, 48, or 72 h at 180 °C (Scheme 1). For comparison, the precursor mixtures were physically mixed without using a grinder. For removing salts (byproduct), the product was washed using H_2O and followed by drying in the air at 80 °C. The effects of heating and grinding time, contents (Si, Al, and Na), additive (NaOH) were tested. For the determination of thermal stability, the as-synthesized products were heated for 6 h at 550 °C. The silica and alumina source concentrations were adjusted to determine the content effects. The synthesized mordenite catalysts were characterized to determine the optimal synthesis procedure and confirm the formation of products. It was found that the mordenite and ZSM-5 zeolites were successfully synthesized by a ball milling approach without using an organic template at 50 min. The amount of sodium plays a significant role (as structure-directing) in the formation of zeolite crystallization. The crystalline phase was formed at a higher Na_2O/Al_2O_3 ratio (7–9) and a lower ratio, the amorphous phase was formed.[33] It is concluded, the high energy ball milling is an effective approach for the synthesis of mordenite and ZSM-5 zeolites at higher Na_2O/Al_2O_3 ratio and

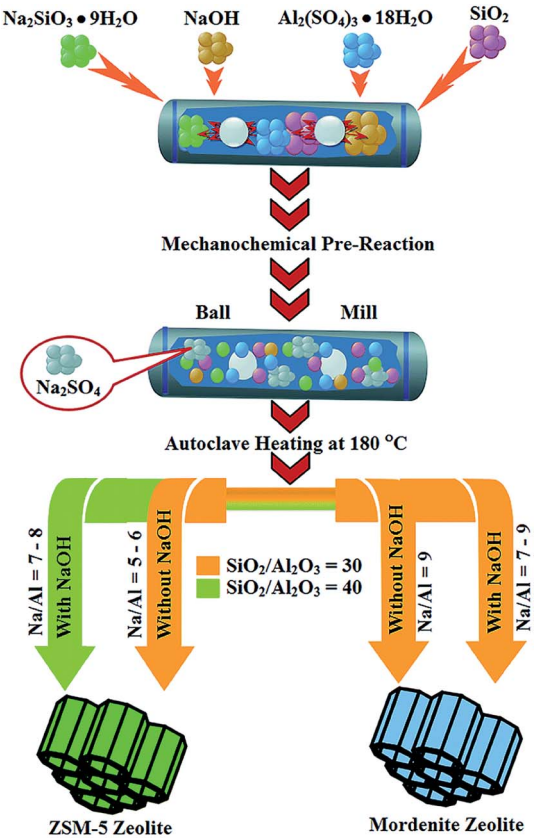

Scheme 1 Graphical summary of key reactions steps used.[33]

efficient catalysts in the biomass conversion. Recently, Kornas and his collaborators synthesized mordenite zeolite without using solvent by automated milling activation and compared with the hydrothermal approach and manual grinding. It was concluded, only 5% of water is enough in automated milling activation which is comparatively lesser than the traditional synthesis of mordenite.[37] It was concluded, the formation of the mordenite phase takes place only in automated milling activation and not in manual milling which is confirmed X-ray diffraction results.

Ultrafast, organic structure-directing agent-free synthesis

At the end of 2016, Zhu *et al.* synthesized mordenite zeolite by an organic structure-directing agent (OSDA)-free, ultrafast approach. They claimed, the mordenite zeolite formed in 10 min, which is comparatively ultrafast to conventional methods.[38] The typical synthesis procedure is explained here. Initially, $NaAlO_2$ (aluminium source) dissolved by NaOH solution (alkali source), subsequently deionized water and 40 wt% LUDOX HS-40 (colloidal silica) for silica source was into the above mixture. Then, at room temperature stirred for 30 min for obtaining a homogenized mixture. Afterward, 10–30 wt% raw micrometer-sized (2 μm) or milled nanometer-sized (200 nm) mordenite seed crystals were added. It was found that micrometer-sized milled mordenite crystals improved the crystallization rate. The reaction mixture was heated at 210 °C in an oil bath (preheated) after feeding inside a tubular reactor. Finally, the tubular heater was cooled down by using water after hydrothermal treatment. The solid product is centrifuged, washed well by using deionized water, and followed by drying in an air oven overnight at 80 °C.[38] The author claimed the mordenite formation was achieved in 10 min (ultrafast). However, the complete crystallization achieved after 30 min (from XRD results), and also the pre-preparation taking some time. Though, we conclude that this approach is faster compared to conventional synthesis. The crystallization time taking more than 6 h, if no seed crystals were added. Hence, mordenite seed crystals (200 nm) played a significant role in the ultrafast synthesis. The same authors were synthesized many zeolite and zeolite-like materials by an ultrafast approach in a few minutes.[39–42]

Piperazine as OSDA

In early 2019, Bai and coworkers synthesized some aluminosilicate zeolites such as ZSM-12, ZSM-5, mordenite, ZSM-35, and ZSM-4 by employing piperazine as OSDA under optimized conditions.[43] For the preparation of $(C_4N_2H_{12})[ZrGe_4O_{10}F_2]$,[44] $[Sn_4(PO_4)_3]$-$0.5[C_4N_2H_{12}]^{2+}$,[45] $(C_4N_2H_{12})U_2O_4F_6$ (MUF-1),[46] aluminophosphates[47] piperazine were used as template. It was also employed in the synthesis of mazzite (MAZ)[48] phillipsite (PHI)[49] zeolites. The author stated that the usage of piperazine as OSDA is found in limited numbers when compared to hexamethylenediamine, piperidine, and pyrrolidine. Hence, the author evaluated the impact of piperazine in the synthesis of aluminosilicates. The author evaluated the impact of Si_2O/Al_2O_3 ratio and reaction time (72 h to 192 h) on zeolite synthesis. The

mordenite and ZSM-4 zeolites were obtained at a low Si_2O/Al_2O_3 ratio (12.8 and 9 respectively). The ZSM-12, ZSM-5, and ZSM-35 zeolites were obtained at a high Si_2O/Al_2O_3 ratio (17.2, 58.7, and 14.3–29.3 respectively). The acidic form of ZSM-35, mordenite, and ZSM-4 catalysts were tested in the reaction of dimethyl ether carbonylation. The high selectivity of methyl acetate is achieved by ZSM-35 and mordenite zeolites. In a typical hydrothermal synthesis, $NaAlO_2$ (2 g), NaOH (0.6 g), H_2O (24 g), and piperazine (12 g) were mixed. In the above solution, Ludox AS-40 (20 g) was introduced into the above solution for gel formation. The contents stirred for 3 h at 40 °C before transferred into a Teflon-lined autoclave. Then, the contents are hydrothermally treated at 150 °C for a particular time (72 h to 192 h). Finally, the filtered synthesized materials dried overnight at 110 °C and then calcinated at 150 °C for 10 h.[43] They concluded, the piperazine was best fitted with the ZSM-35 zeolite (FER-type framework).

Properties of mordenite zeolite

This section discusses the properties of zeolites based on the cell data, building units, pore channels, and framework density. Idealized cell data: orthorhombic, *Cmcm*, $a = 18.3$ Å, $b = 20.5$ Å, $c = 7.5$ Å, secondary building units: 5-1, framework density: 17.2 T/1000 Å^3, crystal chemical data: $|Na_8(H_2O)_{24}|\ [Al_8Si_{40}O_{96}]^-$, MOR channels: [001] 12 6.5 × 7.0 ↔ [001] 8 2.6 × 5.7.

Mordenite mineral, maricopaite [Ga–Si–O]-MOR (interrupted framework), Na-D, Ca-Q, Zeolon (commercial synthetic Zeolon prepared by the Norton company), and LZ-211 have this type of framework. Mordenite is a significant solid acid catalyst. It is used in the isosive process to upgrade the octane number of gasoline and in the alkylation of biphenyl with propene. It belongs to the orthorhombic crystal system (*Cmcm*, $a = 18.3$ Å, $b = 20.5$ Å, $c = 7.5$ Å) and has a framework density of 17.2 T/1000 Å^3. In the mordenite framework, pentasil units are joined to one another *via* common edges to form chains like in the MFI framework. These chains are connected through oxygen bridges to form grooved sheets. It is having 12-ring and 8-ring channels (T-atoms) and runs along the [001] plane with channel dimensions of 6.5 × 7.0 Å and 2.6 × 5.7 Å. Fig. 3 shows the MOR framework type with a basic building block and mordenite mineral.[50–52] The mordenite zeolite pore structure and dimensions are displayed in Fig. 4.

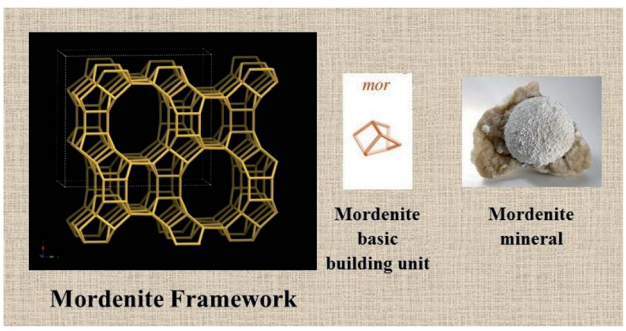

Fig. 3 The mordenite (MOR) framework type, basic building block, and mineral (source for mordenite framework: International Zeolite Association (IZA)).

Optical properties

In 2019, Serykh *et al.* investigated the indium-exchanged mordenite zeolites' optical properties through photoluminescence and UV-Vis diffuse reflectance spectroscopy. The exchanged indium cations in mordenite capable of exhibiting similar intensities of visible-light photoluminescence and ultraviolet emissions. They concluded the visible-light photoluminescence and ultraviolet emission are related to the clusters/oligomers of indium cation (excited state) and isolated indium cations respectively. In addition, indium-exchanged zeolite photoluminescence properties could be tuned by adjusting the space between indium cations.[53] The new finding of optical properties of mordenite zeolite exchanged by cations could be useful in finding wide-ranging applications in the construction of photonic materials.

Recent applications of mordenite zeolite

Recently mordenite zeolite is used in various applications such as electrochemical detection, isomerization, carbonylation, hydrodeoxygenation, *etc.* discussed in the upcoming sections. The overview of the application of mordenite zeolite is displayed in Table 2.

Electrochemical detection

Mercury and other heavy metals are toxic and causing environmental pollution. They enter into the human through water and food. Even a small amount of mercury ions causes various problems in humans such as thyroid problem, kidney failure, damages to the central nervous system.[54,55] At present, a variety of analytical methods are utilized to detect Hg^{2+} ions, for instance, optical sensors,[56–60] atomic fluorescence spectrometry (AFS), X-ray fluorescence spectrometry (XFS), atomic absorption spectrometry (AAS), gas chromatography (GC), *etc.*[61–63] The above methods have high sensitivity and selectivity. Though they are expensive, high operating costs, require sample

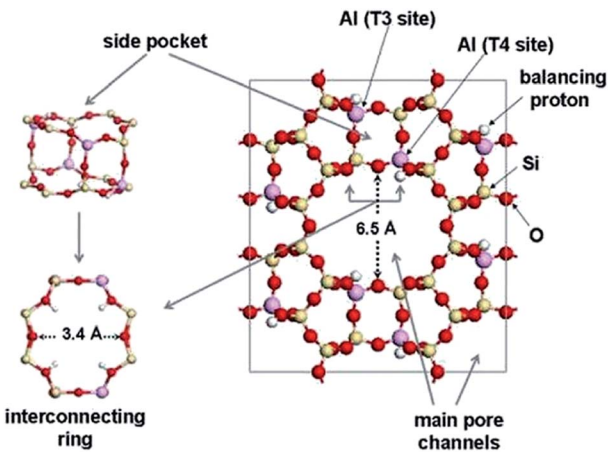

Fig. 4 The mordenite zeolite pore structure and dimensions.

Table 2 Overview of applications of mordenite zeolite

S. no.	Reaction	Catalyst	Reactant	Product	Ref.
1	Electrochemical detection	Platinum incorporated mordenite zeolite modified glassy carbon electrode	Mercury ions	—	56
		Lanthanum-modified mordenite zeolite electrode	Pb(II) and Cd(II) ions	—	57
		Phosphate-modified zeolite carbon paste electrodes	Thiocyanate	—	59
2	Isomerization	Dealuminated mordenite	*n*-Pentane, *n*-hexane, and light naphtha	Isoalkanes, octane number improvement for light naphtha	69
		Hierarchical mordenite	α-Pinene	Camphene, limonene and α-terpinene	70
3	Carbonylation	Hot-water pretreated H-mordenite	Dimethyl ether	Methyl acetate	87
		Hierarchical porous H-mordenite		Methyl acetate	88
		Alkali treated mordenite		Methyl acetate, methanol and light hydrocarbons	90
4	Hydrodeoxygenation	Ru metal supported on ZSM-5, mordenite, COK-12, β-zeolite, Y-zeolite, TiO_2, and ZrO_2	2-Methoxy phenol	Cyclohexane	106
		Ru metal supported on ZSM-5, mordenite, COK-12, β-zeolite, Y-zeolite, TiO_2 and ZrO_2	*m*-Cresol	Methylcyclohexane	107
		Nickel phosphide supported on sodium form of mordenite zeolite	Palm oil	C15–C18 (major) C4–C14 (minor)	108
5	Adsorption	Natural mordenite–clinoptilolite zeolites	CO_2	Adsorbed CO_2 gas	113
		Natural and cation-exchanged clinoptilolite, mordenite and chabazite	H_2	Adsorbed H_2 gas	125
6	Biomass conversion	Hierarchical mordenite zeolites	Biomass (glucose, fructose, cellulose, and bamboo sawdust)	Levulinic acid, humins	138
7	Antibacterial activity	Fe_3O_4@MOR@CuO core–shell	*Staphylococcus aureus* and *Escherichia coli*	—	150
8	Photocatalysis	Fe_3O_4@MOR@CuO core–shell	Methylene blue	Gaseous CO_2 and inorganic ions	163
		Mordenite zeolite@MCM-41			164
		AgBr/Ag_2CO_3–MOR composite		Degraded products	165
9	Fuel cell	Nafion/mordenite composite membrane	Methanol	Energy	171
		Graphene oxide@Nafion–mordenite composite membrane			172
		Sulfonic acid-functionalized zeolites (ZSM-5, beta, mordenite)	Gases (H_2 and O_2)		176
10	Polymerization	High-silica mordenite	Phenylacetylene	Polymerized product	181

pretreatment, follow critical protocol, and for analysis require more amount of sample. Hence, inexpensive, highly selective detection of heavy metal ions is of greater importance. At the same time, electroanalytical methods that have positive aspects for instance high selectivity, rapid analysis, portability, low price for operation, and minimal sample pre-treatment have been explored and documented.[64–72]

However, only a few articles found which is related to the detection of heavy metal ions using the electrochemical approach and mordenite. Sakthinathan *et al.* developed platinum loaded-dealuminated mordenite zeolite decorated modified glassy carbon electrode. It is applied in the electrochemical detection of mercury. The GCE/Pt/D-mordenite electrode show excellent selectivity, reproducibility, higher sensitivity (11.2598 μA μM^{-1} cm^{-2}), and excellent detection limit (3.4 nM). They also compared long linear range with various other electrodes for the determination of mercury ions and found a wider long linear range of 0.1–220 μM.[73] Hence, the detection of heavy metal ions using zeolite support is still open for many zeolites and heavy metal ions.

In 2018, a lanthanum-modified zeolite carbon paste electrode was synthesized by Ismail *et al.* and investigated in the electrochemical detection of heavy metal ions (Pb(II) and Cd(II)). The lanthanum concentration varied (2%, 5%, and 10%) by keeping the mordenite SiO_2/Al_2O_3 ratio as 15. The 2 wt% lanthanum impregnated electrode gave a better response toward the detection of Pb(II) ion. The detection limit for a single detection of Pb(II) was 0.23 ppb. The detection limits in

simultaneous detection of Pb(II) and Cd(II) ions were found to be 0.24 and 0.12 ppb, respectively. They claimed that this electrode is capable of trace heavy metals quantification present in drinking water.[74]

Thiocyanate from industrial effluents with high concentration causes considerable toxicity to aquatics. Its detection is therefore the most significant research objective.[75] Idris *et al.* synthesized mordenite zeolite carbon paste electrodes modified by phosphorous with various ratios of graphite to phosphate zeolite. A various percentage (0 to 20%) of P-MOR was loaded with a constant amount of graphite (30%). The ability of mordenite and phosphate modified zeolite electrochemical detection evaluated towards thiocyanate using cyclic voltammetry for the first time. They found from NMR, the addition of phosphoric acid influences the framework of mordenite and were getting dealuminated. The mordenite carbon paste electrode containing 5% phosphorous demonstrated a maximum current density of 5.6 105 μA cm^{-2} with a linear dynamic range of 10 to 150 μM was obtained.[76] Even in the past, only a few articles found on the electrochemical detection using zeolite. Hence, the detection of various heavy metal ions, toxic chemicals, pathogens using zeolite support is still open for mordenite zeolites.

Isomerization

We already know, isomerization is a process that alters the molecular arrangement of the products without adding or removing anything from the original molecule. In particular, conversion of straight-chain reactant molecule into a branched-chain product molecule.[77] In a refinery industry, it is a significant reaction. The improvement of the high octane number performed by lube stocks (C20–C60), diesel (C18–C26), *n*-paraffins isomerization in jet fuel, and light naphtha isomerization is performed to reduce the pour point as well as plugging point of the oils.[78–80] The catalyst utilized in the above reactions will be bifunctional processes, the first and second components are acid function metallic function respectively.[81] The catalysts used in isomerization of commercial light naphtha are Pt/chloride alumina,[82] Pt/mordenite and Pt/sulphated-zirconia.[83,84] Even though Pt/chloride alumina requires less temperature. It suffers from leaching of Cl. Zeolites-based catalysts are advantageous in this aspect. Mordenite is a superacid solid catalyst and a choice among three catalysts in relation to the generation of a strong level of Brønsted acidity.[85] Tamizhdurai and his collaborators prepared platinum-loaded dealuminated mordenite (various dealumination times – 0.5, 1.0, and 3.0 h) from commercial mordenite and evaluated its catalytic performance in the *n*-hexane, *n*-pentane, and light naphtha isomerization by changing various reaction parameters. At low temperature, the dealuminated mordenite (1.0 h; SiO_2/Al_2O_3 ratio of 40) showed better conversion and selectivity compared to parent and other dealuminated mordenite catalysts. They also compared their catalysts performance with the other isomerization catalysts such as Pt/ZSM-5, Pt/Pd-beta zeolite, Zr-SBA-15, *etc.*, and claimed *n*-pentane and *n*-hexane conversions are comparatively higher than the rest of the catalyst. In addition to that, they performed density functional theory (DFT) calculation and concluded that the *n*-hexane isomerization activation energy is higher than the *n*-pentane isomerization.[86]

More recently, isomerization of α-pinene carried out by Liu *et al.* using hierarchical mordenite zeolite prepared by the microwave-assisted alkaline treatment approach. It was stated, the alkaline-treated mordenite (microwave irradiated) possesses a higher external surface area than parent and alkaline-treated mordenite (conventionally heated). As a result, the conversion of α-pinene is higher (94.7%) than the other two. Also, the selectivity and yield of camphene and limonene are higher. Parent mordenite showed only 46.1% α-pinene conversion. Even though the conversion of conventionally heated mordenite (93.4%) is close to microwave irradiated mordenite (94.7%), the selectivity of limonene is low. The selectivity of camphene, limonene, and α-terpinene are higher with microwave irradiated mordenite. In addition, they performed recycling performance for microwave irradiated mordenite catalyst. They found the conversion is unaffected after 3 cyclic tests. Whereas, a slight decrease in the selectivity of camphene and limonene was observed.[87]

The non-noble metals supported on mordenite towards isomerization reactions can be explored. In recent, catalytic isomerization of galactose into tagatose using Mg–Al hydrotalcite and D-glucose to D-fructose performed by BEA-type zeolite catalysts, which can be explored by mordenite.[88,89]

Carbonylation

Carbonylation is a process of introducing carbon monoxide into an organic molecule. A few articles were found on the topic of carbonylation of dimethyl ether. The carbonylation of dimethyl ether is a more important reaction in recent years. Because the ethanol can be prepared from dimethyl ether. Ethanol has drawn global attention in current years, among the many promising alternatives for fossil fuel resources because of its exceptional properties.[90–95] The traditional synthesis process of ethanol has some drawbacks such as high cost and pollution.[96] A newer and effective ethanol synthesis approach is immediately needed.[97–99] In recent times, the synthesis of ethanol through a greener approach has received significant consideration particularly through carbonylation of dimethyl ether (DME).[100,101] Still, the catalytic performance and consistency of the catalysts towards carbonylation of dimethyl ether must be significantly enhanced. Initially, dimethyl ether converted into methyl acetate by the carbonylation process. Then methyl acetate is converted into ethanol by hydrogenation process.[102,103] Here we can discuss some of the literature related to carbonylation reaction using mordenite zeolite. In 2019, Zhao and his collaborators prepared mordenite zeolite which was pretreated with hot water for different durations (5, 10, or 15 min) to improve catalytic performance. They used these catalysts in the carbonylation of dimethyl ether. Compared to the H-MOR catalyst, the water pretreated catalysts showed better conversion and selectivity. Out of the three pretreated catalysts, the catalyst treated for 10 minutes showed superior conversion and selectivity. The excess treatments of hot water (15 min) inhibit the carbonylation of dimethyl ether. They concluded the

pretreatment of catalysts by hot-water can create more Brønsted acid sites (medium strong and strong) in the catalysts. As a result, the carbonylation of dimethyl ether can be boosted.[104] In another article, Sheng *et al.* explained the carbonylation of dimethyl ether can also be done by hierarchical mordenite zeolite prepared by the hydrothermal method using soft templates (*n*-butylamine and polyacrylamide). They also prepared mordenite zeolite without soft templates for comparison purposes. Based on the characterization results, they stated, there are two types of rings (8 and 12 membered rings) present. The 8 membered rings having more Brønsted sites and framework aluminium present in large numbers which can be responsible for better dimethyl ether conversion and product selectivity. The 12 membered rings having less acidity and responsible for suppressing coke formation. The lower acidity in 12 membered rings is achieved after the introduction of a soft template. By using GC-MS analysis, the authors analyzed the spent catalyst after a reaction time of 10 h and found cyclenes species, methylbenzene species, and some bulky polycyclic aromatics. A large amount of cyclenes and methylbenzene species found in parent mordenite and as a result experiences more coke formation.[105] In 2018, Liu and his researchers examined the roles of 8 and 12 membered ring by using DFT calculation and molecular simulations. Based on the results, they concluded the carbonylation reaction can be improved by the diffusion dynamics alongside reaction kinetics. This can be useful in the design and optimization of catalytic processes.[106]

Wang *et al.* stated that the performance of carbonylation of dimethyl ether can be enhanced after the mordenite catalysts involved in alkaline treatment. They prepared mordenite catalysts with and without the presence of templates. They found the crystallinity decreases, whereas a specific surface area and pore volume increases. On the other hand, the micropores were destroyed and strong acid sites were removed in a considerable amount in the case of without using a template. In conclusion, both the alkaline treatment and templates are responsible for enhancing the carbonylation reaction.[107] The various carbonylation reactions such as hydroformylation, decarbonylation, oxidative carbonylation, and other reactions using mordenite catalyst still need to be explored.

Hydrodeoxygenation

Hydrodeoxygenation is a process of removing oxygen from oxygen-containing compounds. For example, the conversion of oxygenated bio-oil upgradation into valuable fuels/chemicals. The process getting much importance because many valuable materials, for instance, fine chemicals, resins, polymers can be obtained from hydrodeoxygenation of aromatic oxygenates.[108,109] The noble metal loaded solid catalysts having neutral and acidic support, for instance, Mo, Ni, Rh, Ru, Pt, Pd[110–119] as well as bi-metallic catalysts CoMo, Ni–Mo, Ni–Cu[120–122] have been utilized for the hydrodeoxygenation of oxygenates (derived from lignin) for the formation of alkanes, arenas, allene, and alcohols. The materials' performance is highly affected by metal nanoparticles. Hence, it is necessary to find a suitable catalyst for the hydrodeoxygenation reaction. More recently, Dang *et al.*, carried out hydrodeoxygenation of 2-methoxy phenol using Ru metal supported on ZSM-5, mordenite, COK-12, β-zeolite, Y-zeolite, TiO_2, and ZrO_2. These catalysts were purchased commercially and used without modification for creating additional pores. The COK-12 is the only catalyst prepared in the lab. The highest conversion and cyclohexane selectivity was noticed with Ru/ZSM-5 catalyst followed by Ru/mordenite and other catalysts. After the catalytic screening, they performed the rest of the reaction only with Ru/ZSM-5 catalyst. Hence, the Ru/mordenite catalyst was not completely analyzed by Dang *et al.* Though, their research finding with mordenite will be useful for future research. The selectivity of cyclohexane is slightly lower in Ru/mordenite (657 μmol gm^{-1}) compared to Ru/ZSM-5 catalyst. This is due to the high acidic nature of mordenite that can be deactivated rapidly and as a result, coke formed easily compared to Ru/ZSM-5 catalyst (532 μmol gm^{-1}). Hence, the synthesis of a catalyst with hierarchical pore structures would be beneficial.[123] In 2020, conversion of *m*-cresol converted into methylcyclohexane through hydrodeoxygenation process using ruthenium-based catalyst supported on ZSM-5, mordenite, COK-12, β-zeolite, Y-zeolite, TiO_2 and ZrO_2 done by Kumar *et al.* These catalysts were purchased commercially and used without modification except COK-12. The Ru/ZSM-5 catalyst showed superior catalyst activity and TOF followed by Ru/mordenite > Ru/β-zeolite > Ru/γ-zeolite > Ru/TiO_2 > Ru/ZrO_2 > Ru/COK12 > ZSM-5. Hence, they have chosen Ru/ZSM-5 is the best catalytic system and used further in the rest of the hydrodeoxygenation reaction.[124] In the above two reactions, the Ru/ZSM-5 catalyst only studied throughout the process. Also, it should be noted that the noble metal ruthenium is only used in both reactions. Hence, the above two reactions using synthesized hierarchical mordenite zeolite with some other noble and non-noble metal is still needed to be explored more.

Another interesting reaction of hydrodeoxygenation of palm oil using nickel phosphide supported on sodium form of mordenite zeolite carried out by Rakmae and his researchers. In Thailand, palm oil is produced in large quantities and can be used as a biofuel feedstock by hydrodeoxygenation process. At the optimum reaction condition (425 °C, 50 bar), a complete conversion with high selectivity of linear C15–C18 alkanes (green diesel). Also, the obtained liquid product is clear. In addition, the isoparaffins were also found in the liquid product.[125] This research finding making the interest in utilizing available feedstock as biofuels.

Adsorption

We know adsorption is a surface phenomenon and the interest in adsorption of gases growing rapidly. Adsorption of gases using activated carbon materials was carried out extensively and the focus now shifts also to zeolites.[126–129] Releasing carbon dioxide into the environment by electricity generation, industrial operations, and transportation leads to the cause of climate change. Hence, it should have captured before releasing it into the environment.[130] A variety of carbon dioxide capture techniques have already been suggested which may be categorized into seven groups: (1) biological processes, (2) cryogenic

separation, (3) membrane separation, (4) molecular sieves, (5) water scrubber (6) chemical absorption, (7) pressure swing adsorption.[131–134] On a commercial scale, carbon dioxide absorption methods utilizing chemical solutions are mostly applied. But, still more suitable material and technique required for efficient adsorption of carbon dioxide. Recently few articles found on the adsorption of gases using mordenite zeolite. Wahono *et al.* have reported enhanced adsorption of CO_2 natural mordenite–clinoptilolite zeolites. The performance of microporous materials is restricted due to their pore size is smaller. Hence, they have modified the corresponding zeolite by way of acid treatment (1, 3, 6, 9, and 12 M HCl) followed by calcination at high-temperature (400 °C). The mordenite–clinoptilolite zeolite treated with 12 M HCl possesses a large specific surface area (179.44 $m^2\ g^{-1}$) compared to untreated (25.95 $m^2\ g^{-1}$) and other acid-treated materials. At 25 °C and 1 bar pressure, the zeolite treated with 12 M HCl showed a CO_2 adsorption capacity of 0.954 mmol g^{-1}. The CO_2 adsorption capacity increases to 1.35 mmol g^{-1} at 0 °C and 1 bar pressure. Whereas, at 0 °C and 30 bar pressure the zeolite showed a maximum CO_2 adsorption capacity of 5.22 mmol g^{-1}.[130] The utilization of cost-effective natural zeolite as CO_2 adsorbent opened a new application to mordenite.

As the reserves of fossil fuels continue to decline, it is becoming increasingly necessary to find alternative fuels. Hydrogen is considered an alternative to fossil fuels because of its high availability and no air pollution. The problem with storing large amounts of hydrogen in the cylinder is there and research on storing hydrogen becomes more important.[135] There are numerous investigations associated with the adsorption of hydrogen on natural zeolites.[136–141] Though, investigations on adsorption of hydrogen on synthesized and cation exchanged natural zeolites are still inadequate especially mordenite zeolite. In 2019, Alver and Sakızcı have researched on adsorption of hydrogenates at 77 K using natural and various cation-exchanged (H^+, Na^+, K^+, Li^+, Ca^{2+}, and Mg^{2+}) chabazite, clinoptilolite, and mordenite zeolite. Out of the three samples investigated chabazite showed maximum hydrogen adsorption capacity of 0.474 to 1.082 wt%, compared to mordenite and clinoptilolite have 0.224 to 0.337 wt% and 0.065 to 0.555 wt% respectively. The Na exchanged chabazite showed the maximum hydrogen adsorption (1.082 wt%) out of the 21 candidates. This can be due to the natural chabazite possess a BET surface area of 446 $m^2\ g^{-1}$, which is comparatively higher than natural mordenite (68 $m^2\ g^{-1}$) and clinoptilolite (42 $m^2\ g^{-1}$).[142] It is concluded that the structure and pore nature of zeolite plays a critical role in the adsorption of hydrogen. Hence, tailoring the pore properties of mordenite can make a more suitable candidate in adsorption.

Biomass conversion

In recent years, the conversion of biomass into valuable chemicals getting increasingly important in the research area. Because, biomass is abundant, inexpensive, and easily accessible raw materials. The lignin, cellulose, and hemicellulose are three main components of biomass.[143] The 5-hydroxymethylfurfural (5-HMF), levulinic acid (LA), and lactic acid (LAC) can be obtained from cellulose materials. U.S. Energy Department recognized levulinic acid among the platform chemicals.[144] Several heterogeneous catalysts such as HZSM-5,[145] HY zeolite,[146] ionic liquid encapsulated zeolites,[147] Sn-beta,[148] Amberlyst 70,[149] SAC13, ZrO_2,[150] and niobium oxides[151] have been examined towards the conversion of cellulose to levulinic acid. But, these catalysts are suffering from a few drawbacks for instance low yields, low conversion,[152] reaction times are longer,[153] need of costly and harmful solvents, as well as deactivation caused by the formation of humins.[153,154]

Velaga *et al.* have stated the conversion of biomass (glucose, fructose, cellulose, and bamboo sawdust) into levulinic acid using hierarchical mordenite zeolites synthesized by a hydrothermal approach. By changing hydrothermal time (17 h and 34 h) and aging time (0 h and 12 h), the acidic site concentration, mesoporosity, and crystallinity of mordenite significantly increased. The concentration of the Brønsted acid site was found to be higher (112 μmol g^{-1}) than others. The biomass conversion reaction carried at Teflon lined autoclave reactor. The yield of levulinic acid is found maximum (61%) which is converted from bamboo sawdust followed by cellulose, glucose, and fructose are 56, 52, and 43% respectively using hierarchical mordenite catalyst. Besides, humins (carbon-based macromolecular substances) are also formed along with the levulinic acid. The author stated, the formation of humins can be from the intermediates (5-hydroxymethylfurfural and 2,5-dioxo-6-hydroxy-hexanal). They also provided a mechanism for the conversion of biomass to levulinic acid and humins.[155] Alam and his collaborators mentioned the list of biologically- and chemically-derived top chemicals produced from biomass, which is shown in Fig. 5.[156] Hence, a wide range of platform chemicals can be obtained from biomass and broad research can be done using mordenite and other zeolites. In 2017, we have published a paper which is related to biomass conversion (polyols such as sorbitol and xylitol to hydrocarbons) using hierarchical ZSM-5 zeolites, which is still open for mordenite zeolite.[157]

Biological properties (antibacterial activity)

We already know zeolites can be used in a large number of applications. In addition to that, it can also be used for biological applications.[158] For example, clinoptilolite proved useful anti-fungal and anti-bacterial[159] agents, wound treatment,[160] and

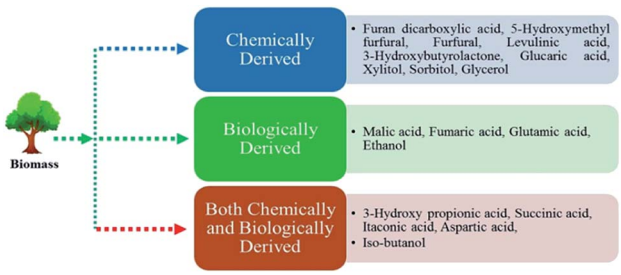

Fig. 5 List of chemically- and biologically-derived top chemicals produced from biomass.

anticancer therapy.[161] Zeolite A and ZSM 5 are applied in quick identification of diseases.[162] Zeolites for instance ZSM 5 and zeolite X are widely utilized as bio-medical implants,[163] hemoperfusion, anesthesiology, and haemodialysis.[158] Zeolite Y, X, and P are employed as drug carriers.[158] Silver-loaded zeolites have been served as anti-microbial agents.[158] The utilization of mordenite towards biological applications needs to be explored more. Even though metal oxides are extensively studied for various biological applications, they have very low or no surface area. Hence, the magnetic metal oxide nanoparticles (Fe_2O_3) can be used as support. Because by using the magnetic field it can be easily separated from the reaction medium. But, generally, they aggregate because of their magnetic attraction and hence they need to be separated.[164,165] Coating with zeolites can suppress the aggregation of magnetic nanoparticles. Because, zeolites have more chemical stability, non-toxicity and the surface can be modified easily.[166] In 2018, Rajabi and Sohrabnezhad, fabricated Fe_3O_4@MOR@CuO core–shell by direct calcination and investigated for its antibacterial properties. The Fe_3O_4@MOR@CuO core–shell showed better antibacterial activity against *Staphylococcus aureus* and *Escherichia coli* compared to CuO and Fe_3O_4@CuO. Besides, it should be noted Fe_3O_4 and Fe_3O_4@MOR not show any antibacterial activity. It is concluded, the CuO antibacterial activity enhanced after loaded with Fe_3O_4@MOR.[167] The same authors, used similar material (Fe_3O_4@MOR@CuO core–shell) as photocatalyst which we will discuss in the next section. Hence, the mordenite zeolite can be used as a support for various metal oxides and can be tested against microbes and viruses. In 2018, Jesudoss *et al.* carried out *in vitro* anti-cancer activity (human lung epithelial cell lines (A549)) by hierarchical ZSM-5 zeolites modified by M (Cu, Ni) first time and showed higher cytotoxicity.[168] Therefore, it is concluded the mordenite might be more suitable against cancer cells.

Photocatalysis

When dyes and harmful chemicals are discharged from the factory, they affect the environment. For example, methylene blue dye can be highly toxic, carcinogenic, and mutagenic when mixed with water.[169] The advanced oxidation process is a powerful oxidation process for the oxidation of a wide range of aqueous organic contaminants.[170] Hence, a large number of metal oxide semiconductors are applied as a photocatalyst, because of its suitable band positions, nontoxic nature, high stability, inexpensive, and simple convenience.[171–175] The performance of the catalyst can be improved by loading on porous, large surface area supports for example alumina,[176] porous carbon,[177] zeolites,[178] graphene oxide.[179] There are only a few articles related to photocatalysis using mordenite zeolite. Not most recently, but a few years back (2017), Rajabi and Sohrabnezhad synthesized Fe_3O_4@MOR@CuO core–shell by direct calcination and utilized as visible light photocatalyst in the degradation of methylene blue. In the previous section, we saw the similar authors used this material in antibacterial activity. From UV-Vis diffuse reflectance spectra, it is found that the Fe_3O_4@CuO show absorption between 300 to 500 nm only. Whereas, theFe_3O_4@MOR@CuO catalyst shows a strong absorption between 400 to 800 nm which will be helpful for increasing the absorption in the visible region. As expected, the Fe_3O_4@MOR@CuO catalyst superior photocatalytic activity than CuO, Fe_3O_4, Fe_3O_4@CuO, as well as Fe_3O_4@MOR towards the degradation of methylene blue. This might be due to the mordenite zeolite have a large surface area and hence more amount of methylene blue can be absorbed and also act as an electron acceptor and transferred to the Fe_3O_4. Hence, to achieve optimal degradation of methylene, all three components are necessary. The photocatalytic efficiency of Fe_3O_4@MOR@CuO catalyst was maintained even after six runs. They varied the dye concentration between 3.2 to 10 ppm and a catalyst amount of 0.05 to 2 g L^{-1}. However, the catalyst found effective up to 5 ppm only with a catalyst amount of 0.9 g L^{-1} at pH 10.[180] A large amount of catalyst (0.9 g L^{-1}) and reaction time (120 min) should be minimized, a maximum of 5 ppm dye concentration needs to be improved.

In a similar period, Sohrabnezhad *et al.* synthesized the mordenite core and put inside the MCM-41 shell. Then Ag and ZnO nanoparticles were incorporated and tested photocatalytic efficiency towards the degradation of methylene blue under visible light. Diffuse reflectance recorded for Ag/ZnO–MOR@MCM-41, the ZnO NPs, Ag/ZnO, and MOR@MCM-41 samples. All the samples show absorption characteristics. But, Ag/ZnO and Ag/ZnO–MOR@MCM-41 only show absorption even in the visible region. Hence, these two candidates are most suitable in the visible region. However, the Ag/ZnO–MOR@MCM-41 catalyst shows superior dye degradation (92%) and decolorization (97.24%) of methylene blue. However, Ag/ZnO without support shows only 33.15% degradation and 42.50% decolorization of dye. Even Ag/ZnO–MOR (55.20%) and Ag/ZnO–MCM-41 (79.52%) unable to attain maximum conversion. They varied the dye concentration between 3.2 to 20 ppm and a catalyst amount of 0.03 to 0.1 g L^{-1}. The catalyst found effective upto 10 ppm only with a catalyst amount of 0.08 g L^{-1} at pH 6.5 in 60 min.[164] Though, the performance of catalysts was found better with respect to catalyst amount, time, and dye concentration compared to a work described in the previous section. It should be noted the efficiency of photocatalyst can be improved in the visible region after the deposition of silver. Hence, silver plays an important role in the absorption of visible light in a large fraction. As stated in the previous section, this author also claimed better absorption of MCM-41 and an electron acceptor of mordenite improved the dye degradation efficiency by Ag/ZnO–MOR@MCM-41 catalyst. They claimed the efficiency of a photocatalyst not decreased even after four recycles.[181] From the above two research work, we conclude that the mordenite zeolite can be prepared as a core–shell and applied in the photocatalytic degradation of pollutants. The performance of mordenite is found superior when used as a core than as a shell from the above discussions. Also, a variety of dyes, drugs, phenols, and chlorophenols can be analyzed by mordenite zeolite along with photocatalyst.

Asadollahi *et al.* prepared and incorporated Ag_2CO_3 (silver carbonate) nanoparticles in mordenite zeolite by precipitation method. A different weight percentage of AgBr (silver bromide – 20%, 40%, and 50%) coupled with Ag_2CO_3–mordenite. The

synthesized catalysts photocatalytic performance tested against degradation of methylene blue under visible light. The AgBr/Ag_2CO_3–MOR composite with 50% AgBr showed higher photocatalytic degradation efficiency of methylene blue. The efficiency of AgBr/Ag_2CO_3–MOR composite compared with the Ag_2CO_3 and Ag_2CO_3–MOR catalysts. The following parameters varied such as, catalyst amount (0.1 to 1.0 g without adjusting pH), amount of AgBr (20%, 40%, and 50%), (1 ppm to 10 ppm) and from the parameters the optimum support amount, catalyst amount, AgBr amount, dye concentration and time are 0.2 g L^{-1}, 0.7 g L^{-1}, 50 wt%, 3.2 ppm, and 75 min respectively. The author claimed the reason for the better efficiency of AgBr/Ag_2CO_3–MOR composite is the mordenite adsorb more methylene blue molecule and also acts as an electron acceptor. The 90% degradation and 95% decolorization of methylene blue achieved in 75 min for AgBr (50 wt%)/Ag_2CO_3–MOR catalyst.[182] Overall from the above discussions, if the mordenite catalyst used as a core show better photocatalytic performance. Also, if the hierarchical pore structured mordenite is used, the efficiency will be higher with less amount of catalyst.

Fuel cell

As the demand for energy is increasing daily in the world, its use is increasing. As fossil fuels continue to decline, we are forced to look for alternative sources of energy.[183,184] Direct methanol fuel cell (DMFC) gaining attention because of its clean energy, easy to use, and high energy efficiency.[185–187] Prapainainar *et al.* extensively studied DMFC using mordenite with various materials.[188–191] Hence, we will discuss here only two from the most recent one. In 2020, Prapainainar *et al.* have published a research article related to the evaluation of the effect of the solvent (alcohol) ratio on DMFC performance of ion/mordenite composite membrane fabricated with a solution casting approach.[188] Nafion is a fluoropolymer–copolymer and a brand name for sulfonated tetrafluoroethylene discovered by Walther Grot.[192] The amount (ratio) of alcohol changed between 0 to 5 (0, 1, 3, 5) by comparing the volume of DMF. They thought decreasing the ratio of alcohol might increase the ratio of composite membrane homogeneity, but an undesirable effect (two layers of polymer and mordenite formed) happens. Also, the composite membrane chemical resistance was reduced due to increased solubility when the ratio of alcohol decreased. At 343.15 K, the composite membrane having an alcohol volume ratio of 5 reaches a maximum power density of 11.5 mW cm^{-2} compared to other composite membranes at 2 M concentration of methanol.[188] The same author in 2019 for improving the performance of Nafion–mordenite composite membranes and decreasing the methanol permeability by incorporating graphene oxide. At 30, 50, and 70 °C, silane grafted Nafion–mordenite composite with 0.05% content of graphene oxide showed the highest proton conductivity of 0.0560, 0.0738, and 0.08645 S cm^{-1} respectively than silane grafted silane–mordenite composite without graphene and recast Nafion. In addition, it possesses the lowest methanol permeability in comparison with the others.[189]

In 2019, Munavalli and Kariduraganavar developed the sulfonic acid functionalized zeolites (ZSM-5, beta, mordenite) for fuel cell applications. Various parameters such as proton conductivity, ion exchange capacity, water uptake, and swelling behavior in relation to mass% (4, 8, and 12) of functionalized materials to determine the performance of membranes. The zeolites with 8% functionalized material to show the highest ion exchange capacity revealed from the data of proton conductivity. The functionalized Na-mordenite zeolite, Na-beta zeolite, and Na-ZSM-5 zeolite composite membranes show the corresponding proton conductivity of 0.124, 0.112, and 0.102 S cm^{-1}. Also, the zeolites with 8% functionalized material possess outstanding power density of 0.45 W cm^{-2} at 1.1 A cm^{-2}, 0.42 W cm^{-2} at 1.05 A cm^{-2}, and 0.37 W cm^{-2} at 1.1 A with respect to Na-mordenite zeolite, Na-beta zeolite, and ZSM-5 zeolite composite membranes from the studies of fuel cell performance. They concluded these functionalized composite materials show superior performance than the Nafion 117 commercial membrane and can be a promising material in fuel cell applications.[193] This fuel cell application with mordenite zeolite will gain more importance due to energy demand. Also, there are various types of fuel cells that can be explored by mordenite.

Polymerization

Polymerization is one of the most important chemical reactions and catalyzed by various catalysts. The polymerization of phenylacetylene catalyzed by various metal loaded complexes and attracts more due to its unique properties, for instance, conductivity, humidity sensor, non-linear optical properties, ferromagnetism, and oxygen permeability.[194–197] Although polymerization of phenylacetylene was not tried by zeolite catalysts. In 2020, Confalonieri *et al.* investigated phenylacetylene polymerization using high-silica mordenite with high pressure for the first time. At high pressure conditions, the monomeric phenylacetylene is inserted into a mordenite zeolite. In a combination of zeolite pores, high pressure, and temperature, the monomeric phenylacetylene converted into oligomeric species having a high proportion of conjugation. The formation of polymeric material was confirmed by X-ray diffraction and infrared spectroscopy analysis. Based on the IR data, they suggest at 0.30 GPa a slow oligomerization reaction seen, and also a large number of monomeric phenylacetylene species was found at 0.30 GPa. The complete polymerization of phenylacetylene observed when the applied pressure reaches to ~1.10 GPa. Besides, a higher temperature is required for further reactivity. The pressure reaches 2.58 GPa when it is kept in an oven for 5 h at 150 °C. Whereas, the pressure reaches 1.35 GPa when the samples quench at room temperature. They concluded this research will open a new path for finding novel composite materials having exciting optoelectronic properties through polymerization of aromatic molecules with the help of pressure and zeolite frameworks.[198]

Biomass valorization

The per capita per day global food consumption provides a key input variable to understand the related biomass

accumulation related to food production alone. The global food consumption was 2358 kcal in the 1960s and the same increased to about 3000 kcal in 2020. The migration of people towards urban cities has increased manifold, and the near absence of natural biodegradation in urban habitats has demanded technological solutions to sustainable waste management techniques. The collections, preparation, transformation to value-added products provide opportunities to exploit these waste products.

Biomass feedstocks, including bagasse, vegetable oils, cooking oil, as well as several biomass intermediates, are potential resources for conversion to biofuel. Factors, such as complex composition impede the conversion of biomass to obtain valuable products. Accordingly, processing biomass to liquid fuel requires a series of steps and conditions.[199] The continued development achieved in the preceding years in evolving the properties of zeolite catalysts to mitigate the challenges related to biomass up-gradation. The potential of customizing the vital physicochemical properties has provided the option of utilizing the zeolites for biomass valorization. The promising application pathways reviewed in this work are catalytic pyrolysis and hydroprocessing of biomass. The introduction of hierarchical zeolites have further enhanced the catalytic reactions to produce higher yield and selectivity.

The pyridine adsorbed HMOR zeolite was studied in the carbonylation of DME, and it was observed that pyridine influenced the selectivity of reaction sites to ensure higher stability of the catalyst.[200] Ethanol synthesis has been attempted from syngas feedstock, HMOR modified with Zn improved the catalytic performance by improving the selectivity from 7.4% to 69%; however, to avoid deactivation Zn-HMOR was subsequently modified with pyridine.[201] Alkaline treatment generated mesopore mordenite catalyst with varying Si/Al ratio was used in the pyrolysis and catalytic treatment of vacuum gas oil, which produced less yield but higher quality oil.[202] Catalytic pyrolysis using proton forms of mordenite was attempted in the conversion of pine wood biomass, and it was observed that ketones and phenols formed the major groups of elements in the biofuel.[203] Hydrothermal process utilizing mordenite zeolite catalysts possessing mesoporous structure displayed more of an aluminium framework and Brønsted acidic sites, which produced methyl acetate (MA) from dimethyl ether (DME).[105] The sourcing of hydrogen for the hydrogenation of biomass has been a challenge to its viable implementation, but the possibility of utilizing H_2 derived from renewable sources has thrown open the chances for a cost-effective solution.[204] Catalyst transfer hydrogenation (CTH) enables the up-gradation of biomass-derived fuels and the production of valuable chemicals.[205] Hydrogenolysis of cyclic ethers and polyols were attempted by utilizing zeolite supported Ni phyllosilicate catalyst, and the yield amounts were highest for ZSM-5, but MOR yielded higher than beta supports.[206]

Post-consumer plastic upgradation to fuel

Synthetic plastics are non-biodegradable and cause extensive harm to the entire ecosystem. The persistent pollutants transform over the years to micro and nanoplastics, which facilitates their entry into every living thing. The solution to mitigate plastic pollution is to convert them to valuable products through pyrolysis. Zeolites display a vital role in the valorization of post-consumer synthetic plastics. Catalytic cracking has been more effective than the thermal cracking of plastic solid waste. Catalytic pyrolysis reactions take place at a much lower temperature and at the same time, ensure higher yield.

Catalytic pyrolysis of low-density polyethylene (LDPE) has been attempted by employing an H-MOR catalyst, and it was observed that the cracked products were in the carbon range of C1–C19.[207] Mordenite catalysts employed in catalytic cracking of LDPE have provided yields (40%) higher than thermal cracking.[208] Mordenite catalyst has been an effective catalyst in the conversion of plastic solid waste to liquid fuel. Though its yield performance has been recorded as lower than other zeolites, its selectivity in producing high-quality oil makes it a valuable pyrolysis catalyst. Catalytic pyrolysis experiments of raw pyrolysis wax oil were conducted utilizing various zeolites (including mordenite), and it was observed that mordenite yield was lower, but it produced the highest yield of paraffin.[209]

Conclusion

The latest advancement of mordenite zeolite synthesis approaches in the past few years has given new impetus to utilizing this product. The primary reason for the increased interest in mordenite zeolite was the use of inexpensive silicon sources (rice husk ash and waste coal fly ash) and aluminium source (metakaolin and faujasite zeolite) respectively. In addition to that, the synthesis was also carried out without the use of costly organic templates like TEA^+ cation or making use of cheap mixed organic templates such as (glycerol (GL), ethylene glycol (EG), and polyethylene glycol 200 (PEG)). Finally, the discussed synthesis approaches taken few days for crystallization time with effective crystallinity and pore size. From the discussion, it is concluded that the synthesis of mordenite zeolite using cheap sources will have a great opportunity in the production of catalysts and as a replacement for the materials synthesized using costly templates.

From the novel applications of mordenite zeolite in catalysis, it is expected to expand over the next few years. The medical and industrial sector requires low-cost sensors for detecting heavy metal. The construction of the mordenite zeolite-based electrode will become a promising electrochemical sensor of heavy metals. The ability of mordenite zeolite as an isomerization catalyst result may find tremendous opportunities in the petroleum refinery industry. The bio-oil up gradation (hydrodeoxygenation) using mordenite catalysts create new opportunities for complete utilization of lignin-derived oxygenated aromatic compounds, which can produce valuable chemicals. The mordenite zeolite can be a suitable candidate for the adsorption of CO_2 and possible applications in the conversion of CO_2 into chemicals and also adsorption of H_2 and possible applications in hydrogen storage. In biomedical applications, there is a scope for mordenite zeolite in further development (antimicrobial and anticancer activity). In photocatalytic

degradation of dyes, the efficiency of catalyst depends upon the adsorption of more dye molecules which was achieved by mordenite zeolite as support and it can be a promising candidate in various photocatalytic applications. Based on the discussions, the mordenite zeolite is definitely an ideal material for fuel cell applications. Even though the mordenite is used in various novel applications, there is some potential application such as plastic pyrolysis, NO_x removal, polyols to hydrocarbon conversions yet to be explored by mordenite zeolite.

Abbreviations

AAS	Atomic absorption spectrometry
BEA	Zeolite beta
BET	Brunauer–Emmett–Teller
C16NMP	*N*-Cetyl-*N*-methylpyrrolidinium
DFT	Density functional theory
DME	Dimethyl ether
DMF	Dimethylformamide
DMFC	Direct methanol fuel cell
EG	Ethylene glycol
FAU	Faujasite
FER	Ferrierite
GC	Gas chromatography
GCE	Glassy carbon electrode
GC-MS	Gas chromatography-mass spectrometry
GL	Glycerol
HMF	5-Hydroxymethylfurfural
HR-TEM	High-resolution transmission electron microscopy
IUPAC	International Union of Pure and Applied Chemistry
LA	Levulinic acid
LAC	Lactic acid
MOR	Mordenite
MFI	Mordenite framework inverted
NMR	Nuclear magnetic resonance
OSDA	Organic structure-directing agent
PEG	Polyethylene glycol 200
RHA	Rice husk ash
RPM	Revolutions per minute
TPA^+ cation	Tetrapropylammonium cation
XFS	X-ray fluorescence spectrometry
XRF	X-ray fluorescence
ZSM-5	Zeolite socony mobil-5

Conflicts of interest

The authors declare that there is no conflict of interest regarding the publication of this paper.

Acknowledgements

The authors are thankful to Prof. S. Sivasanker for his guidelines and constant support for carrying out the review paper and thank Prof. B. Viswanathan NCCR, IIT-Madras for providing laboratory and workplace.

Notes and references

1 P. Anastas and N. Eghbali, *Chem. Soc. Rev.*, 2010, **39**, 301–312.
2 J. Zhao, Y. Yin, Y. Li, W. Chen and B. Liu, *Chem. Eng. J.*, 2016, **284**, 405–411.
3 C. Perego and R. Millini, *Chem. Soc. Rev.*, 2013, **42**, 3956–3976.
4 N. Giri, M. G. Del Pópolo, G. Melaugh, R. L. Greenaway, K. Rätzke, T. Koschine, L. Pison, M. F. C. Gomes, A. I. Cooper and S. L. James, *Nature*, 2015, **527**, 216–220.
5 X. Fan and Y. Jiao, in *Sustainable Nanoscale Engineering*, ed. G. Szekely and A. Livingston, Elsevier, 2020, pp. 115–137, DOI: 10.1016/B978-0-12-814681-1.00005-9.
6 S. A. A. Nakhli, M. Delkash, B. E. Bakhshayesh and H. Kazemian, *Water, Air, Soil Pollut.*, 2017, **228**, 464.
7 A. Poursaeidesfahani, E. Andres-Garcia, M. de Lange, A. Torres-Knoop, M. Rigutto, N. Nair, F. Kapteijn, J. Gascon, D. Dubbeldam and T. J. H. Vlugt, *Microporous Mesoporous Mater.*, 2019, **277**, 237–244.
8 Y. Li, L. Li and J. Yu, *Chem*, 2017, **3**, 928–949.
9 C. G. S. Lima, N. M. Moreira, M. W. Paixão and A. G. Corrêa, *Current Opinion in Green and Sustainable Chemistry*, 2019, **15**, 7–12.
10 G. J. Millar, S. J. Couperthwaite and K. Alyuz, *J. Environ. Chem. Eng.*, 2016, **4**, 1918–1928.
11 G. J. Millar, A. Winnett, T. Thompson and S. J. Couperthwaite, *J. Water Process Eng.*, 2016, **9**, 47–57.
12 J. Wen, H. Dong and G. Zeng, *J. Cleaner Prod.*, 2018, **197**, 1435–1446.
13 A. Alkhlel and H. de Lasa, *Ind. Eng. Chem. Res.*, 2018, **57**, 13627–13638.
14 H. Valpotic, *Period. Biol.*, 2017, **119**, 159–172.
15 S. Montalvo, L. Guerrero, R. Borja, E. Sánchez, Z. Milán, I. Cortés and M. Angeles de la laRubia, *Appl. Clay Sci.*, 2012, **58**, 125–133.
16 S. Rezvantalab and F. Bahadori, *Asian J. Agric. Res.*, 2015, **9**, 343–349.
17 C. Li, M. Moliner and A. Corma, *Angew. Chem., Int. Ed.*, 2018, **57**, 15330–15353.
18 M. Ranocchiari and J. A. v. Bokhoven, *Phys. Chem. Chem. Phys.*, 2011, **13**, 6388–6396.
19 R. Bingre, B. Louis and P. Nguyen, *Catalysts*, 2018, **8**, 163.
20 G. D. Gatta and P. Lotti, in *Modified Clay and Zeolite Nanocomposite Materials*, ed. M. Mercurio, B. Sarkar and A. Langella, Elsevier, 2019, pp. 1–25, DOI: 10.1016/B978-0-12-814617-0.00001-3.
21 A. Godelitsas, P. Gamaletsos and M. Roussos-Kotsis, *Eur. J. Mineral.*, 2010, **22**, 797–811.
22 E. M. Flanigen, in *Stud. Surf. Sci. Catal.*, ed. H. van Bekkum, E. M. Flanigen, P. A. Jacobs and J. C. Jansen, Elsevier, 2001, vol. 137, pp. 11–35.
23 A. N. C. van laak, R. W. Gosselink, S. L. Sagala, J. D. Meeldijk, P. E. de Jongh and K. P. de Jong, *Appl. Catal., A*, 2010, **382**, 65–72.

24 M. Niwa, N. Katada and K. Okumura, *Characterization and Design of Zeolite Catalysts*, 2010.
25 M. A. Klunk, S. B. Schröpfer, S. Dasgupta, M. Das, N. R. Caetano, A. N. Impiombato, P. R. Wander and C. A. M. Moraes, *Chem. Zvesti*, 2020, **74**, 2481–2489.
26 M. Costa and A. Araujo, *Rev. Propr. Ind.*, 2010, **2083**, 76.
27 H. M. Lankapati, D. R. Lathiya, L. Choudhary, A. K. Dalai and K. C. Maheria, *ChemistrySelect*, 2020, **5**, 1193–1198.
28 D. R. Lathiya, D. V. Bhatt and K. C. Maheria, *ChemistrySelect*, 2019, **4**, 4392–4397.
29 G. J. Kim and W. S. Ahn, *Zeolites*, 1991, **11**, 745–750.
30 E. A. Abdelrahman, R. M. Hegazey and A. Alharbi, *J. Inorg. Organomet. Polym. Mater.*, 2020, **30**, 1369–1383.
31 H. Chen, Y. J. Zhang, P. Y. He and Y. Zhang, *Ferroelectrics*, 2019, **547**, 44–50.
32 A. Bolshakov, D. E. Romero Hidalgo, A. J. F. van Hoof, N. Kosinov and E. J. M. Hensen, *ChemCatChem*, 2019, **11**, 2803–2811.
33 M. H. Nada, S. C. Larsen and E. G. Gillan, *Nanoscale Adv.*, 2019, **1**, 3918–3928.
34 S. L. James, C. J. Adams, C. Bolm, D. Braga, P. Collier, T. Friščić, F. Grepioni, K. D. M. Harris, G. Hyett, W. Jones, A. Krebs, J. Mack, L. Maini, A. G. Orpen, I. P. Parkin, W. C. Shearouse, J. W. Steed and D. C. Waddell, *Chem. Soc. Rev.*, 2012, **41**, 413–447.
35 A. Karmakar, M. S. Dodd, X. Zhang, M. S. Oakley, M. Klobukowski and V. K. Michaelis, *Chem. Commun.*, 2019, **55**, 5079–5082.
36 A. O. Atoyebi and C. Brückner, *Inorg. Chem.*, 2019, **58**, 9631–9642.
37 A. Kornas, J. E. Olszówka, M. Urbanova, K. Mlekodaj, L. Brabec, J. Rathousky, J. Dedecek and V. Pashkova, *Eur. J. Inorg. Chem.*, 2020, **2020**, 2791–2797.
38 J. Zhu, Z. Liu, A. Endo, Y. Yanaba, T. Yoshikawa, T. Wakihara and T. Okubo, *CrystEngComm*, 2017, **19**, 632–640.
39 Z. Liu, T. Wakihara, D. Nishioka, K. Oshima, T. Takewaki and T. Okubo, *Chem. Mater.*, 2014, **26**, 2327–2331.
40 Z. Liu, T. Wakihara, D. Nishioka, K. Oshima, T. Takewaki and T. Okubo, *Chem. Commun.*, 2014, **50**, 2526–2528.
41 Z. Liu, N. Nomura, D. Nishioka, Y. Hotta, T. Matsuo, K. Oshima, Y. Yanaba, T. Yoshikawa, K. Ohara, S. Kohara, T. Takewaki, T. Okubo and T. Wakihara, *Chem. Commun.*, 2015, **51**, 12567–12570.
42 Z. Liu, T. Wakihara, C. Anand, S. H. Keoh, D. Nishioka, Y. Hotta, T. Matsuo, T. Takewaki and T. Okubo, *Microporous Mesoporous Mater.*, 2016, **223**, 140–144.
43 L. Bai, Z. Xiong, E. Zhan, S. Li and W. Shen, *J. Mater. Sci.*, 2019, **54**, 7589–7602.
44 Z. Liu, L. Weng, Y. Zhou, Z. Chen and D. Zhao, *J. Mater. Chem.*, 2003, **13**, 308–311.
45 Y.-L. Liu, G.-S. Zhu, J.-S. Chen, L.-Y. Na, J. Hua, W.-Q. Pang and R.-R. Xu, *Inorg. Chem.*, 2000, **39**, 1820–1822.
46 P. S. Halasyamani, S. M. Walker and D. O'Hare, *J. Am. Chem. Soc.*, 1999, **121**, 7415–7416.
47 X. Tong, J. Xu, C. Wang, H. Lu, P. Huang, W. Yan, J. Yu, F. Deng and R. Xu, *Microporous Mesoporous Mater.*, 2012, **155**, 153–166.
48 H. Xu, P. Dong, L. Liu, J. G. Wang, F. Deng and J. X. Dong, *J. Porous Mater.*, 2007, **14**, 97–101.
49 Q. Shi, H. Xu, J. Li, Z. Lin and J. Dong, *Microporous Mesoporous Mater.*, 2009, **121**, 152–157.
50 Z. Ma, J. Xie, J. Zhang, W. Zhang, Y. Zhou and J. Wang, *Microporous Mesoporous Mater.*, 2016, **224**, 17–25.
51 S. K. Wahono, A. Suwanto, D. J. Prasetyo, Hernawan, T. H. Jatmiko and K. Vasilev, *Appl. Surf. Sci.*, 2019, **483**, 940–946.
52 L. B. McCusker and C. Baerlocher, in *Stud. Surf. Sci. Catal.*, ed. J. Čejka, H. van Bekkum, A. Corma and F. Schüth, Elsevier, 2007, vol. 168, pp. 13–37.
53 A. I. Serykh, *Microporous Mesoporous Mater.*, 2019, **275**, 147–151.
54 P. Rameshkumar, P. Viswanathan and R. Ramaraj, *Sens. Actuators, B*, 2014, **202**, 1070–1077.
55 N. Ratner and D. Mandler, *Anal. Chem.*, 2015, **87**, 7492.
56 S. A. El-Safty, M. A. Shenashen and A. A. Ismail, *Chem. Commun.*, 2012, **48**, 9652–9654.
57 S. A. El-Safty, M. A. Shenashen and A. Shahat, *Small*, 2013, **9**, 2288–2296.
58 M. A. Shenashen, S. A. El-Safty and E. A. Elshehy, *Analyst*, 2014, **139**, 6393–6405.
59 M. A. Shenashen, A. Shahat and S. A. El-Safty, *J. Hazard. Mater.*, 2013, **244–245**, 726–735.
60 A. Aboelmagd, S. A. El-Safty, M. A. Shenashen, E. A. Elshehy, M. Khairy, M. Sakaic and H. Yamaguchi, *Chem.–Asian J.*, 2015, **10**, 2467–2478.
61 N. Bi, Y. Chen, H. Qi, X. Zheng, Y. Chen, X. Liao, H. Zhang and Y. Tian, *Sens. Actuators, B*, 2012, **166–167**, 766–771.
62 A. Giacomino, O. Abollino, M. Malandrino and E. Mentasti, *Talanta*, 2008, **75**, 266–273.
63 M. Behzad, M. Asgari, M. Shamsipur and M. G. Maragheh, *J. Electrochem. Soc.*, 2013, **160**, B31–B36.
64 R. N. Goyal, V. K. Gupta and S. Chatterjee, *Sens. Actuators, B*, 2010, **149**, 252–258.
65 A. Salmanipour and M. A. Taher, *J. Solid State Electrochem.*, 2011, **15**, 2695–2702.
66 G. K. Raghu, S. Sampath and M. Pandurangappa, *J. Solid State Electrochem.*, 2012, **16**, 1953–1963.
67 I.-M. Simionca, A. Arvinte, R. Ardeleanu and M. Pinteala, *Electroanalysis*, 2012, **24**, 1995–2004.
68 S. Intarakamhang, W. Schuhmann and A. Schulte, *J. Solid State Electrochem.*, 2013, **17**, 1535–1542.
69 L. Pinto and S. G. Lemos, *Electroanalysis*, 2014, **26**, 299–305.
70 P. S. Adarakatti and P. Malingappa, *J. Solid State Electrochem.*, 2016, **20**, 3349–3358.
71 M. R. Ganjali, M. Asgari, F. Faridbod, P. Norouzi, A. Badiei and J. Gholami, *J. Solid State Electrochem.*, 2010, **14**, 1359–1366.
72 S. Morante-Zarcero, D. Pérez-Quintanilla and I. Sierra, *J. Solid State Electrochem.*, 2015, **19**, 2117–2127.

73 S. Sakthinathan, P. Tamizhdurai, A. Ramesh, T.-W. Chiu, V. L. Mangesh, S. Veerarajan and K. Shanthi, *Microporous Mesoporous Mater.*, 2020, **292**, 109770.
74 A. Ismail, A. Kawde, O. Muraza, M. A. Sanhoob, M. A. Aziz and A. R. Al-Betar, *Arabian J. Sci. Eng.*, 2019, **44**, 217–226.
75 A. Badri and P. Pouladsaz, *Int. J. Electrochem. Sci.*, 2011, **6**, 3178–3195.
76 A. Idris, T. A. Saleh, M. A. Sanhoob, O. Muraza and A.-R. Al-Betar, *J. Taiwan Inst. Chem. Eng.*, 2017, **72**, 236–243.
77 N. P. Cheremisinoff and M. B. Haddadin, in *Beyond Compliance*, ed. N. P. Cheremisinoff and M. B. Haddadin, Gulf Publishing Company, 2006, pp. 1–77, DOI: 10.1016/B978-0-9765113-9-7.50005-5.
78 C. Martínez and A. Corma, *Coord. Chem. Rev.*, 2011, **255**, 1558–1580.
79 B. Ducourty, G. Szabo, J. P. Dath, J. P. Gilson, J. M. Goupil and D. Cornet, *Appl. Catal., A*, 2004, **269**, 203–214.
80 S. V. Konnov, I. I. Ivanova, O. A. Ponomareva and V. I. Zaikovskii, *Microporous Mesoporous Mater.*, 2012, **164**, 222–231.
81 A. Chica, A. Corma and P. J. Miguel, *Catal. Today*, 2001, **65**, 101–110.
82 A. de Lucas, P. Cañizares and A. Durán, *Appl. Catal., A*, 2001, **206**, 87–93.
83 T. Kimura, *Catal. Today*, 2003, **81**, 57–63.
84 R. M. Jao, T. B. Lin and J. R. Chang, *J. Catal.*, 1996, **161**, 222–229.
85 C. A. Henriques, A. M. Bentes, P. Magnoux, M. Guisnet and J. L. F. Monteiro, *Appl. Catal., A*, 1998, **166**, 301–309.
86 P. Tamizhdurai, A. Ramesh, P. S. Krishnan, S. Narayanan, K. Shanthi and S. Sivasanker, *Microporous Mesoporous Mater.*, 2019, **287**, 192–202.
87 Y. Liu, D. Zheng, B. Li, Y. Lyu, X. Wang, X. Liu, L. Li, S. Yu, X. Liu and Z. Yan, *Microporous Mesoporous Mater.*, 2020, **299**, 110117.
88 P. Drabo and I. Delidovich, *Catal. Commun.*, 2018, **107**, 24–28.
89 M. M. Antunes, D. Falcão, A. Fernandes, F. Ribeiro, M. Pillinger, J. Rocha and A. A. Valente, *Catal. Today*, 2021, **362**, 162–174.
90 L. D. Schmidt and P. J. Dauenhauer, *Nature*, 2007, **447**, 914–915.
91 P. Lu, G. Yang, Y. Tanaka and N. Tsubaki, *Catal. Today*, 2014, **232**, 22–26.
92 Q. Cheng, Y. Tian, S. Lyu, N. Zhao, K. Ma, T. Ding, Z. Jiang, L. Wang, J. Zhang, L. Zheng, F. Gao, L. Dong, N. Tsubaki and X. Li, *Nat. Commun.*, 2018, **9**, 3250.
93 Y. Zhang, X. San, N. Tsubaki, Y. Tan and J. Chen, *Ind. Eng. Chem. Res.*, 2010, **49**, 5485–5488.
94 Q. Wei, G. Yang, X. Gao, L. Tan, P. Ai, P. Zhang, P. Lu, Y. Yoneyama and N. Tsubaki, *Chem. Eng. J.*, 2017, **316**, 832–841.
95 Q. Qian, M. Cui, J. Zhang, J. Xiang, J. Song, G. Yang and B. Han, *Green Chem.*, 2018, **20**, 206–213.
96 J. J. Spivey and A. Egbebi, *Chem. Soc. Rev.*, 2007, **36**, 1514–1528.
97 Z. Zhang, N. Zhao, K. Ma, Q. Cheng, J. Zhang, L. Zheng, Y. Tian and X. Li, *Chin. Chem. Lett.*, 2019, **30**, 513–516.
98 Z. Cheng, S. Huang, Y. Li, J. Lv, K. Cai and X. Ma, *Ind. Eng. Chem. Res.*, 2017, **56**, 13618–13627.
99 S. Wang, W. Guo, L. Zhu, H. Wang, K. Qiu and K. Cen, *J. Phys. Chem. C*, 2015, **119**, 524–533.
100 X. Li, X. San, Y. Zhang, T. Ichii, M. Meng, Y. Tan and N. Tsubaki, *ChemSusChem*, 2010, **3**, 1192–1199.
101 G. Yang, X. San, N. Jiang, Y. Tanaka, X. Li, Q. Jin, K. Tao, F. Meng and N. Tsubaki, *Catal. Today*, 2011, **164**, 425–428.
102 A. A. C. Reule, V. Prasad and N. Semagina, *Microporous Mesoporous Mater.*, 2018, **263**, 220–230.
103 Z. Ren, M. N. Younis, H. Zhao, C. Li, X. Yang, E. Wang and G. Wang, *Chin. J. Chem. Eng.*, 2020, **28**, 1612–1622.
104 N. Zhao, Q. Cheng, S. Lyu, L. Guo, Y. Tian, T. Ding, J. Xu, X. Ma and X. Li, *Catal. Today*, 2020, **339**, 86–92.
105 H. Sheng, W. Qian, H. Zhang, P. Zhao, H. Ma and W. Ying, *Microporous Mesoporous Mater.*, 2020, **295**, 109950.
106 Z. Liu, X. Yi, G. Wang, X. Tang, G. Li, L. Huang and A. Zheng, *J. Catal.*, 2019, **369**, 335–344.
107 X. Wang, R. Li, C. Yu, Y. Liu, L. Zhang, C. Xu and H. Zhou, *Fuel*, 2019, **239**, 794–803.
108 M. V. Bykova, D. Y. Ermakov, V. V. Kaichev, O. A. Bulavchenko, A. A. Saraev, M. Y. Lebedev and V. A. Yakovlev, *Appl. Catal., B*, 2012, **113–114**, 296–307.
109 C. Zhao, S. Kasakov, J. He and J. A. Lercher, *J. Catal.*, 2012, **296**, 12–23.
110 C. Zhao, Y. Kou, A. A. Lemonidou, X. Li and J. A. Lercher, *Angew. Chem., Int. Ed.*, 2009, **48**, 3987–3990.
111 C. Zhao and J. A. Lercher, *ChemCatChem*, 2012, **4**, 64–68.
112 C. Wang, A. V. Mironenko, A. Raizada, T. Chen, X. Mao, A. Padmanabhan, D. G. Vlachos, R. J. Gorte and J. M. Vohs, *ACS Catal.*, 2018, **8**, 7749–7759.
113 R. C. Runnebaum, T. Nimmanwudipong, R. R. Limbo, D. E. Block and B. C. Gates, *Catal. Lett.*, 2012, **142**, 7–15.
114 D. P. Gamliel, S. Karakalos and J. A. Valla, *Appl. Catal., A*, 2018, **559**, 20–29.
115 J. Chang, T. Danuthai, S. Dewiyanti, C. Wang and A. Borgna, *ChemCatChem*, 2013, **5**, 3041–3049.
116 D. Garcia-Pintos, J. Voss, A. D. Jensen and F. Studt, *J. Phys. Chem. C*, 2016, **120**, 18529–18537.
117 F. Yang, H. Wang, J. Han, Q. Ge and X. Zhu, *Catal. Today*, 2020, **347**, 79–86.
118 X. Zhang, T. Wang, L. Ma, Q. Zhang, X. Huang and Y. Yu, *Appl. Energy*, 2013, **112**, 533–538.
119 V. O. O. Gonçalves, C. Ciotonea, S. Arrii-Clacens, N. Guignard, C. Roudaut, J. Rousseau, J.-M. Clacens, S. Royer and F. Richard, *Appl. Catal., B*, 2017, **214**, 57–66.
120 M. V. Bykova, O. A. Bulavchenko, D. Y. Ermakov, M. Y. Lebedev, V. A. Yakovlev and V. N. Parmon, *Catal. Ind.*, 2011, **3**, 15–22.
121 B. Yoosuk, D. Tumnantong and P. Prasassarakich, *Fuel*, 2012, **91**, 246–252.
122 V. N. Bui, D. Laurenti, P. Afanasiev and C. Geantet, *Appl. Catal., B*, 2011, **101**, 239–245.
123 R. Dang, X. Ma, J. Luo, Y. Zhang, J. Fu, C. Li and N. Yang, *J. Energy Inst.*, 2020, **93**, 1527–1534.

124 A. Kumar, A. Kumar, B. Biswas, J. Kumar, S. R. Yenumala and T. Bhaskar, *Renewable Energy*, 2020, **151**, 687–697.
125 S. Rakmae, N. Osakoo, M. Pimsuta, K. Deekamwong, C. Keawkumay, T. Butburee, K. Faungnawakij, C. Geantet, S. Prayoonpokarach, J. Wittayakun and P. Khemthong, *Fuel Process. Technol.*, 2020, **198**, 106236.
126 L. Jiang, A. Gonzalez-Diaz, J. Ling-Chin, A. P. Roskilly and A. J. Smallbone, *Appl. Energy*, 2019, **245**, 1–15.
127 H. Rezvani, S. Fatemi and J. Tamnanloo, *J. Environ. Chem. Eng.*, 2019, **7**, 103085.
128 M. K. Al Mesfer and M. Danish, *J. Environ. Chem. Eng.*, 2018, **6**, 4514–4524.
129 S. Koonaphapdeelert, J. Moran, P. Aggarangsi and A. Bunkham, *Energy Sustainable Dev.*, 2018, **43**, 196–202.
130 S. K. Wahono, J. Stalin, J. Addai-Mensah, W. Skinner, A. Vinu and K. Vasilev, *Microporous Mesoporous Mater.*, 2020, **294**, 109871.
131 E. Ryckebosch, M. Drouillon and H. Vervaeren, *Biomass Bioenergy*, 2011, **35**, 1633–1645.
132 N. Abatzoglou and S. Boivin, *Biofuels, Bioprod. Biorefin.*, 2009, **3**, 42–71.
133 N. Álvarez-Gutiérrez, S. García, M. V. Gil, F. Rubiera and C. Pevida, *Energy Procedia*, 2014, **63**, 6527–6533.
134 D. Andriani, A. Wresta, T. Atmaja and A. Saepudin, *Appl. Biochem. Biotechnol.*, 2014, **172**, 1909–1928.
135 J. Andersson and S. Grönkvist, *Int. J. Hydrogen Energy*, 2019, **44**, 11901–11919.
136 Y. Kawamura, Y. Edao, Y. Iwai, T. Hayashi and T. Yamanishi, *Fusion Eng. Des.*, 2014, **89**, 1539–1543.
137 K.-H. Chung, *Energy*, 2010, **35**, 2235–2241.
138 K. Munakata and Y. Kawamura, *Fusion Sci. Technol.*, 2012, **62**, 71–76.
139 Y. Kawamura, Y. Iwai, K. Munakata and T. Yamanishi, *J. Nucl. Mater.*, 2013, **442**, S455–S460.
140 Y. Kawamura, Y. Edao and T. Yamanishi, *Fusion Eng. Des.*, 2013, **88**, 2255–2258.
141 B. Erdoğan Alver and F. Esenli, *Microporous Mesoporous Mater.*, 2017, **244**, 67–73.
142 B. Erdoğan Alver and M. Sakızcı, *Int. J. Hydrogen Energy*, 2019, **44**, 6748–6755.
143 D. Klemm, B. Heublein, H.-P. Fink and A. Bohn, *Angew. Chem., Int. Ed.*, 2005, **44**, 3358–3393.
144 X. Lin, Q. Huang, G. Qi, S. Shi, L. Xiong, C. Huang, X. Chen, H. Li and X. Chen, *Sep. Purif. Technol.*, 2017, **174**, 222–231.
145 W. Zeng, D.-g. Cheng, H. Zhang, F. Chen and X. Zhan, *React. Kinet. Mech. Catal.*, 2010, **100**, 377–384.
146 N. A. S. Ramli and N. A. S. Amin, *Appl. Catal., B*, 2015, **163**, 487–498.
147 P. Saxena, B. Velaga and N. R. Peela, *ChemistrySelect*, 2017, **2**, 10379–10386.
148 T. C. Acharjee and Y. Y. Lee, *Environ. Prog. Sustainable Energy*, 2018, **37**, 471–480.
149 F. Wang, L. Jiang, J. Wang and Z. Zhang, *Energy Fuels*, 2016, **30**, 5885–5892.
150 S. S. Joshi, A. D. Zodge, K. V. Pandare and B. D. Kulkarni, *Ind. Eng. Chem. Res.*, 2014, **53**, 18796–18805.
151 Y. Liu, H. Li, J. He, W. Zhao, T. Yang and S. Yang, *Catal. Commun.*, 2017, **93**, 20–24.
152 R. Weingarten, W. C. Conner and G. W. Huber, *Energy Environ. Sci.*, 2012, **5**, 7559–7574.
153 W. Weiqi and W. Shubin, *Chem. Eng. J.*, 2017, **307**, 389–398.
154 H. Chen, B. Yu and S. Jin, *Bioresour. Technol.*, 2011, **102**, 3568–3570.
155 B. Velaga, R. P. Parde, J. Soni and N. R. Peela, *Microporous Mesoporous Mater.*, 2019, **287**, 18–28.
156 M. I. Alam, A. Ali, S. Gupta and A. Haider, *Microbial Applications*, Springer, Cham, 2017, vol. 2, pp. 153–166, DOI: 10.1007/978-3-319-52669-0_8.
157 S. Narayanan, J. Judith Vijaya, S. Sivasanker, T. M. Sankaranarayanan, C. Ragupathi, L. John Kennedy, R. Jothiramalingam, H. A. Al-Lohedan and A. M. Tawfeek, *React. Kinet., Mech. Catal.*, 2017, **122**, 247–257.
158 K. Pavelić and M. Hadzija, in *Handbook of Zeolite Science and Technology*, 2003, pp. 1143–1174.
159 K. Pavelić, M. Hadžija, L. Bedrica, J. Pavelić, I. Đikić, M. Katić, M. Kralj, M. H. Bosnar, S. Kapitanović, M. Poljak-Blaži, Š. Križanac, R. Stojković, M. Jurin, B. Subotić and M. Čolić, *J. Mol. Med.*, 2001, **78**, 708–720.
160 Y. Li, L. Hui, L. Xiao, L. Zhou, J. Shentu, X. Zhang and J. Fan, *Materials*, 2012, **5**, 2586–2596.
161 V. Tomečková, M. Reháková, G. Mojžišová, J. Magura, T. Wadsten and K. Zelenáková, *Microporous Mesoporous Mater.*, 2012, **147**, 59–67.
162 Y. L. A. Leung and K. L. Yeung, *Chem. Eng. Sci.*, 2004, **59**, 4809–4817.
163 R. S. Bedi, D. E. Beving, L. P. Zanello and Y. Yan, *Acta Biomater.*, 2009, **5**, 3265–3271.
164 W. Xie and N. Ma, *Energy Fuels*, 2009, **23**, 1347–1353.
165 W. Xie and J. Wang, *Energy Fuels*, 2014, **28**, 2624–2631.
166 J. M. Rosenholm, J. Zhang, W. Sun and H. Gu, *Microporous Mesoporous Mater.*, 2011, **145**, 14–20.
167 S. K. Rajabi and S. Sohrabnezhad, *J. Fluorine Chem.*, 2018, **206**, 36–42.
168 S. K. Jesudoss, J. Judith Vijaya, K. Kaviyarasu, P. IyyappaRajan, S. Narayanan and L. John Kennedy, *J. Photochem. Photobiol., B*, 2018, **186**, 178–188.
169 K. M. Parida and L. Mohapatra, *Chem. Eng. J.*, 2012, **179**, 131–139.
170 X. Li, J. Yu and M. Jaroniec, *Chem. Soc. Rev.*, 2016, **45**, 2603–2636.
171 L. Tian, X. Xian, X. Cui, H. Tang and X. Yang, *Appl. Surf. Sci.*, 2018, **430**, 301–308.
172 X. Meng, Y. Zhuang, H. Tang and C. Lu, *J. Alloys Compd.*, 2018, **761**, 15–23.
173 Y. Zhang, J. Chen, H. Tang, Y. Xiao, S. Qiu, S. Li and S. Cao, *J. Hazard. Mater.*, 2018, **354**, 17–26.
174 Y. Fu, W. Liang, J. Guo, H. Tang and S. Liu, *Appl. Surf. Sci.*, 2018, **430**, 234–242.
175 X. Cui, L. Tian, X. Xian, H. Tang and X. Yang, *Appl. Surf. Sci.*, 2018, **430**, 108–115.
176 P. Borker and R. Desai Gaokar, *Surf. Interfaces*, 2020, **19**, 100477.

177 J. Hu, L. Zhang, B. Lu, X. Wang and H. Huang, *Vacuum*, 2019, **159**, 59–68.
178 R. Chen, C. Yang, Q. Zhang, B. Zhang and K. Deng, *J. Catal.*, 2019, **374**, 297–305.
179 İ. Tanişik, Ö. Uğuz, D. Akyüz, R. M. ZunainAyaz, C. Sarioğlu, F. Karaca, A. R. Özkaya and A. Koca, *Int. J. Hydrogen Energy*, 2020, **45**, 34845–34856.
180 S. K. Rajabi and S. Sohrabnezhad, *Microporous Mesoporous Mater.*, 2017, **242**, 136–143.
181 S. Sohrabnezhad, N. Karkoudi and A. Asadollahi, *Colloids Surf., A*, 2017, **520**, 17–25.
182 A. Asadollahi, S. Sohrabnezhad and R. Ansari, *Adv. Powder Technol.*, 2017, **28**, 304–313.
183 E. Ogungbemi, O. Ijaodola, F. N. Khatib, T. Wilberforce, Z. El Hassan, J. Thompson, M. Ramadan and A. G. Olabi, *Energy*, 2019, **172**, 155–172.
184 J. Zhu, J. Tan, Q. Pan, Z. Liu and Q. Hou, *Energy*, 2019, **189**, 116135.
185 Z. Yuan, W. Fu, Y. Zhao, Z. Li, Y. Zhang and X. Liu, *Energy*, 2013, **55**, 1152–1158.
186 L. Wang, Y. Zhang, Z. An, S. Huang, Z. Zhou and X. Liu, *Energy*, 2013, **58**, 283–295.
187 S. Fang, Y. Zhang, Z. Ma, S. Sang and X. Liu, *Energy*, 2016, **112**, 1015–1023.
188 P. Prapainainar, Z. Du, A. Theampetch, C. Prapainainar, P. Kongkachuichay and S. M. Holmes, *Energy*, 2020, **190**, 116451.
189 P. Prapainainar, N. Pattanapisutkun, C. Prapainainar and P. Kongkachuichay, *Int. J. Hydrogen Energy*, 2019, **44**, 362–378.
190 P. Prapainainar, S. Maliwan, K. Sarakham, Z. Du, C. Prapainainar, S. M. Holmes and P. Kongkachuichay, *Int. J. Hydrogen Energy*, 2018, **43**, 14675–14690.
191 P. Prapainainar, Z. Du, P. Kongkachuichay, S. M. Holmes and C. Prapainainar, *Appl. Surf. Sci.*, 2017, **421**, 24–41.
192 N. Yusoff, in *Graphene-Based Electrochemical Sensors for Biomolecules*, ed. A. Pandikumar and P. Rameshkumar, Elsevier, 2019, pp. 155–186, DOI: 10.1016/B978-0-12-815394-9.00007-8.
193 B. B. Munavalli and M. Y. Kariduraganavar, *Electrochim. Acta*, 2019, **296**, 294–307.
194 D. S. Suslov, M. V. Pakhomova, M. V. Bykov, I. A. Ushakov and V. S. Tkach, *Catal. Commun.*, 2019, **119**, 16–21.
195 M. C. Joseph, A. J. Swarts and S. F. Mapolie, *Dalton Trans.*, 2018, **47**, 12209–12217.
196 P. Zhang, H. Wang, X. Shi, X. Yan, X. Wu, S. Zhang, B. Yao, X. Feng, J. Zhi, X. Li, B. Tong, J. Shi, L. Wang and Y. Dong, *J. Polym. Sci., Part A: Polym. Chem.*, 2017, **55**, 716–725.
197 M. Marigo, N. Marsich and E. Farnetti, *J. Mol. Catal. A: Chem.*, 2002, **187**, 169–177.
198 G. Confalonieri, M. Fabbiani, R. Arletti, S. Quartieri, F. Di Renzo, J. Haines, G. Tabacchi, E. Fois, G. Vezzalini, G. Martra and M. Santoro, *Microporous Mesoporous Mater.*, 2020, **300**, 110163.
199 D. P. Serrano, J. A. Melero, G. Morales, J. Iglesias and P. Pizarro, *Catal. Rev.*, 2018, **60**, 1–70.
200 J. Liu, H. Xue, X. Huang, P.-H. Wu, S.-J. Huang, S.-B. Liu and W. Shen, *Chin. J. Catal.*, 2010, **31**, 729–738.
201 Z. Cao, T. Hu, J. Guo, J. Xie, N. Zhang, J. Zheng, L. Che and B. H. Chen, *Fuel*, 2019, **254**, 115542.
202 S. Stefanidis, K. Kalogiannis, E. F. Iliopoulou, A. A. Lappas, J. M. Triguero, M. T. Navarro, A. Chica and F. Rey, *Green Chem.*, 2013, **15**, 1647–1658.
203 A. Aho, N. Kumar, K. Eränen, T. Salmi, M. Hupa and D. Y. Murzin, *Fuel*, 2008, **87**, 2493–2501.
204 W. Jin, L. Pastor-Pérez, J. Yu, J. A. Odriozola, S. Gu and T. R. Reina, *Current Opinion in Green and Sustainable Chemistry*, 2020, **23**, 1–9.
205 M. J. Gilkey and B. Xu, *ACS Catal.*, 2016, **6**, 1420–1436.
206 E. Soghrati, T. K. C. Ong, C. K. Poh, S. Kawi and A. Borgna, *Appl. Catal., B*, 2018, **235**, 130–142.
207 R. C. Mordi, R. Fields and J. Dwyer, *J. Anal. Appl. Pyrolysis*, 1994, **29**, 45–55.
208 J. Aguado, D. P. Serrano, J. M. Escola and A. Peral, *J. Anal. Appl. Pyrolysis*, 2009, **85**, 352–358.
209 K.-H. Lee and J. Anal, *Appl. Pyrolysis*, 2012, **94**, 209–214.